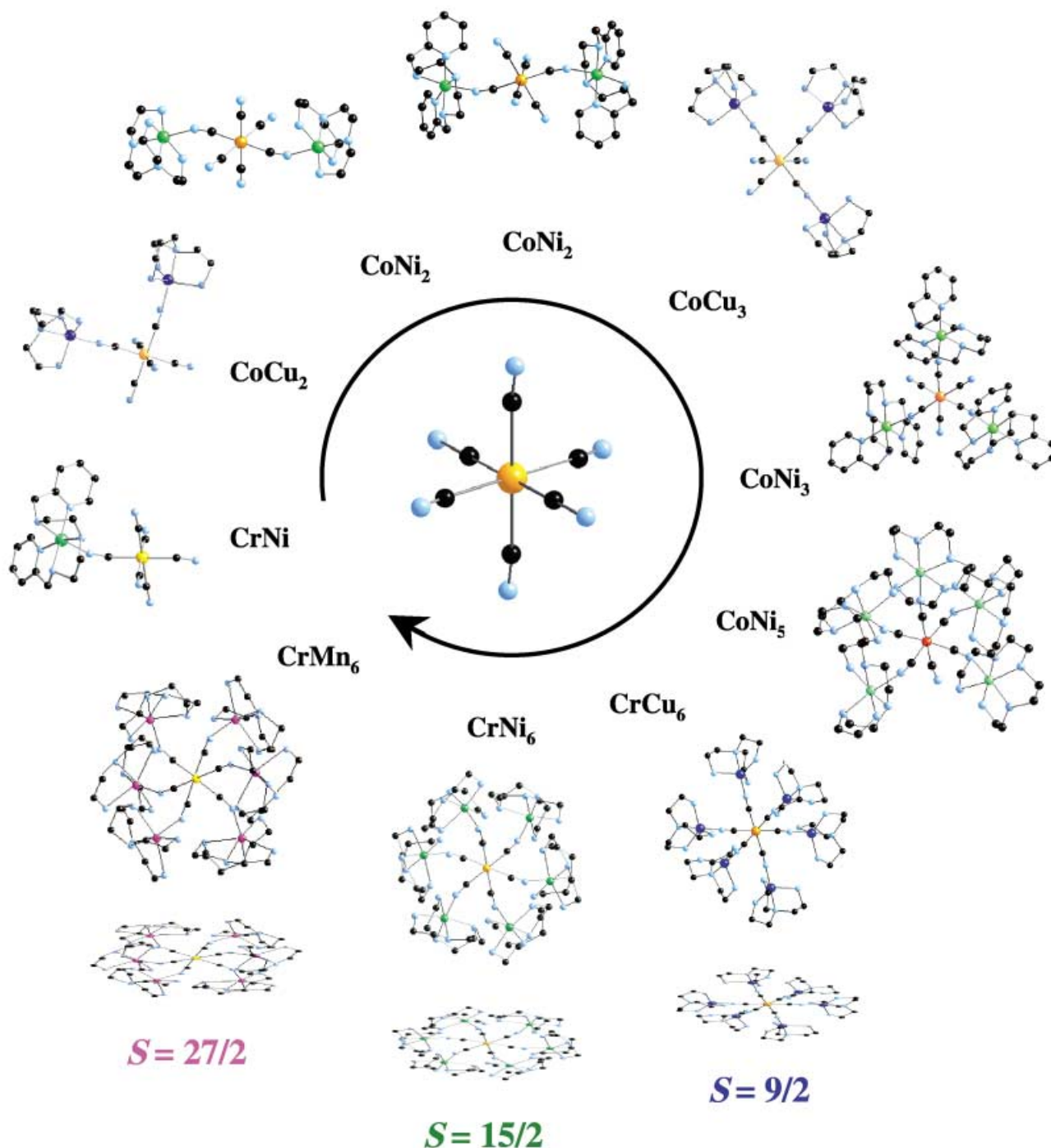


## Hexacyanometalate Molecular Chemistry



# Hexacyanometalate Molecular Chemistry: Heptanuclear Heterobimetallic Complexes; Control of the Ground Spin State\*\*

Valérie Marvaud,<sup>\*[a]</sup> Caroline Decroix,<sup>[a]</sup> Ariane Sculler,<sup>[a]</sup> Carine Guyard-Duhayon,<sup>[a]</sup> Jacqueline Vaissermann,<sup>[a]</sup> Florence Gonnet,<sup>[b]</sup> and Michel Verdaguer<sup>\*[a]</sup>

**Abstract:** Following a bottom-up approach to nanomaterials, we present a rational synthetic route from hexacyanometalates  $[M(CN)_6]^{3-}$  ( $M = Cr^{III}$ ,  $Co^{III}$ ) cores to well-defined heptanuclear complexes. By changing the nature of the metallic cations and using a localised orbital model it is possible to control and to tune the ground state spin value. Thus, with  $M = Cr^{III}$ ,  $d^3$ ,  $S = 3/2$ , three heptanuclear species were built and characterised by mass spectrometry in solution, by single-crystal X-ray diffrac-

tion and by powder magnetic susceptibility measurements,  $[Cr^{III}(CN-M'L_n)_6]^{9+}$  ( $M' = Cu^{II}$ ,  $Ni^{II}$ ,  $Mn^{II}$ ,  $L_n =$  polydentate ligand), showing spin ground states  $S_G = 9/2$  [ $Cu^{II}$ ], with ferromagnetic interactions  $J_{Cr,Cu} = +45 \text{ cm}^{-1}$ ,  $S_G = 15/2$  [ $Ni^{II}$ ] and  $J_{Cr,Ni} = +17.3 \text{ cm}^{-1}$ ,  $S_G = 27/2$  [ $Mn^{II}$ ],

with an antiferromagnetic interaction  $J_{Cr,Mn} = -9 \text{ cm}^{-1}$ , (interaction Hamiltonian  $\mathcal{H} = -J_{Cr,M} [S_{Cr} \sum_i S_M(i)]$ ,  $i = 1-6$ ). With  $M = Co^{III}$ ,  $d^6$ ,  $S = 0$ , the heptanuclear analogues  $[Co^{III}(CN-M'L_n)_6]^{9+}$  ( $M' = Cu^{II}$ ,  $Ni^{II}$ ,  $Mn^{II}$ ) were similarly synthesised and studied. They present a singlet ground state and allow us to evaluate the weak antiferromagnetic coupling constant between two next-nearest neighbours  $M'-Co-M'$ .

**Keywords:** cyanides • high-spin molecules • magnetic properties • polynuclear complexes • single-molecule magnets

## Introduction

Magnets are widely used in a large number of applications and one of the challenges of the next few years will be the use of nanoparticles, or even molecules, as the smallest sized entities for magnetic information storage.<sup>[1]</sup> Particles of various materials in the 10–100 nm range that exhibit slow relaxation of magnetisation below a temperature defined as the blocking temperature have been reported.<sup>[2]</sup> Most of these nanomaterials are obtained from macroscopic samples by decreasing their sizes through the so-called *top-down* approach. To

achieve the same properties, molecular chemists have recently grown polynuclear complexes from mononuclear precursors in the frame of a *bottom-up* approach, and opened the field of “single-molecule magnets”.<sup>[3–5]</sup> Only a few examples of these polynuclear complexes featuring large spins and very peculiar magnetisation properties have already been published, such as  $Mn_{12}$  ( $S = 10$ ),<sup>[6–8]</sup>  $Mn_4$  ( $S = 9/2$ )<sup>[9,10]</sup> and  $Fe_8$  ( $S = 10$ ).<sup>[11,12]</sup>

At low temperature the magnetic moments of these compounds, orientated in the direction of the field, keep aligned when the field is switched off. This property is due to an axial anisotropy due to a zero field splitting (ZFS)  $D$  ( $D$  negative) of the ground state, which gives rise to an energy barrier between the two energetically degenerate  $\pm m_S$  states (Figure 1). The energy of the barrier is equal to  $DS_z^2$ ,  $S_z$  being the projection of the spin ground state on the easy axis.<sup>[3]</sup> Another striking property of these objects, when they present some rhombic anisotropy  $E$ , is magnetic quantum tunnelling.<sup>[13,14]</sup> The magnetic properties of such complexes are now well studied and well known, and the presence of steps in the magnetic hysteresis loop, the quantum tunnelling and the quantum phase interference effects are better understood.<sup>[15]</sup> Nevertheless, a number of questions remain such as the effective control of the blocking temperature and of the parameters involved in the magnetic properties of a single-molecule magnet.

Raising the blocking temperature is undoubtedly one of the most important goals in this new field of single-molecule

[a] Dr. V. Marvaud, Prof. Em. M. Verdaguer, C. Decroix, Dr. A. Sculler, Dr. C. Guyard-Duhayon, Dr. J. Vaissermann  
Laboratoire de Chimie Inorganique et Matériaux Moléculaires, CNRS, UMR 7071  
Université Pierre et Marie Curie  
75252 Paris Cedex 05 (France)  
Fax: (+33)01-44-27-38-41  
E-mail: marvaud@ccr.jussieu.fr

[b] Dr. F. Gonnet  
Laboratoire de Chimie Structurale Organique et Biologique, CNRS, UMR 7613  
Université Pierre et Marie Curie  
75252 Paris Cedex 05 (France)

[\*\*] Hexacyanometalate Molecular Chemistry: for Part 2, see reference [18], for Part 3, see reference [19].

Supporting information for this article is available on the WWW under <http://www.chemed.org> or from the author.

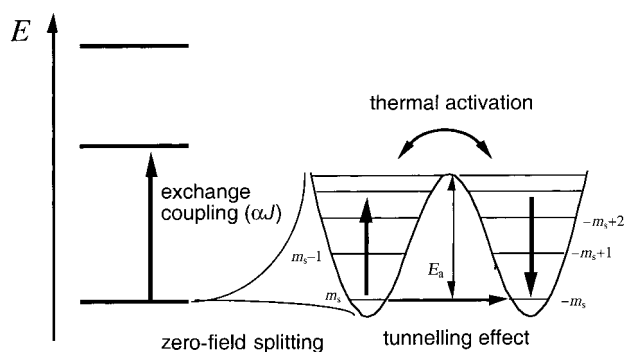


Figure 1. Schematic plot of a single-molecule magnet experiencing axial zero field splitting.

magnets. A trivial calculation demonstrates for example that if one wants to create an anisotropy barrier  $DS_z^2$  able to compete with the thermal quantum at room temperature (let us say 400 K), a possible choice is a spin  $S=20$  and a ZFS constant of the ground state  $D=1$  K. This is one of the first necessary conditions to overcome to be able to store useful information on *one* molecule. This is not in fact a priori an out-of-reach goal. Thus, compounds with a high-spin ground state and large easy axis type of anisotropy are a new challenge in molecular magnetism.<sup>[16, 17]</sup> Another evident requirement is to get a spin ground state well separated in energy from the first excited states, separation that in the simplest cases is proportional to the exchange interaction  $J_{\text{intra}}$  between two neighbouring spin carriers, metallic cations or radicals. The intramolecular  $J$  coupling constants must therefore be as high as possible. Finally, a last condition if one wants to observe the magnetic properties of the isolated polynuclear clusters is to get negligible intermolecular interactions  $J_{\text{inter}}$ .

Our approach is based on a step-by-step synthetic strategy to get polynuclear complexes based on hexacyanometalate chemistry with a good control of the most important parameters ( $S$ ,  $D$ ,  $J$ ,  $zJ$ ). The work is divided into several contributions. The first three are: 1) the synthesis and the study of heptanuclear bimetallic complexes  $[\text{MM}'_6]$  where the ground spin state is controlled by the electronic structure and spin value of  $M$  and  $M'$  (Part 1, present paper); 2) the synthesis and study of polynuclear heterobimetallic complexes with variable stoichiometries,  $[\text{MM}'_x]$  with ( $x=1, 2, 3, 5, 6$ ;  $M'=Ni^{II}$ ) where the structural anisotropy is controlled (Part 2, see following paper in this journal)<sup>[18]</sup> and 3) the synthesis and study of trinuclear complexes  $[\text{MM}'_2]$  where intra- and intermolecular interactions are analysed (Part 3).<sup>[19]</sup> The strategy is presently extended to other polycyanometalate precursors to obtain tailor-made high-spin molecules and single-molecule magnets.

Most of the high-spin molecules described have been obtained by “serendipitous assembly”<sup>[20]</sup> such as the  $\text{Mn}_{12}$ ,<sup>[7–8]</sup> mentioned above, the nickel and cobalt polynuclear cages by Winpenny et al.,<sup>[20, 21]</sup> the  $[\text{Fe}_{17}][\text{Fe}_{19}]$  compounds by Powell et al.,<sup>[22, 23]</sup> and the octacyanometalate clusters published by Hashimoto et al.<sup>[24]</sup> and Decurtins et al.<sup>[25, 26]</sup> Murrie et al. are now adopting a similar approach to produce  $\text{Ni}_{21}$  cages.<sup>[27]</sup> The serendipitous assembly has produced attractive structures but, as shown above, there exists a demand for a rational design of

clearly identified target molecules. In this perspective, our process is therefore different, based on a rational approach tending towards effective control of the chemistry.

After presenting the synthetic strategy that has been used in this study, we shall discuss the synthesis, the main characterizations and the magnetic properties of three complexes  $[\text{Cr}^{III}(\text{CN}-\text{M}'\text{L}_n)_6]^{9+}$  ( $M'=Cu^{II}, Ni^{II}, Mn^{II}$ ,  $L_n$  = polydentate ligand), denoted as  $\text{CrCu}_6$ ,  $\text{CrNi}_6$  and  $\text{CrMn}_6$ , respectively. Additional discussion will focus on the cobalt(III)-centred analogues, with  $M'=Cu^{II}, Ni^{II}, Mn^{II}$ , denoted as  $\text{CoCu}_6$ ,  $\text{CoNi}_6$  and  $\text{CoMn}_6$ .

**Synthetic strategy:** Hexacyanometalate chemistry has been developed in the laboratory for the design and synthesis of room-temperature molecule-based magnets.<sup>[28–30]</sup> These precursors have also been used in molecular chemistry for the formation of high spin polynuclear complexes. Two communications dealt with the two heptanuclear complexes  $[\text{Cr}(\text{CN}-\text{Ni}(\text{tetren}))_6(\text{ClO}_4)_9]$ ,<sup>[31]</sup> (with ligand tetraethylenepentamine, tetren) denoted as  $\text{CrNi}_6^*$  in the following, and  $[\text{Cr}(\text{CN}-\text{Mn}(\text{trispicmeen}))_6(\text{ClO}_4)_9]$ ,<sup>[32]</sup> (with ligand  $N,N,N'$ -(tris(2-pyridylmethyl)- $N'$ -methylethane)-1,2-diamine, trispicmeen) denoted as  $\text{CrMn}_6^*$ , which were not fully characterised: 1) for  $\text{CrNi}_6^*$ , the full determination of the crystal structure proved to be impossible (even at low temperature and using a CCD detector) and we never succeeded in reaching a magnetisation at saturation equal to the expected 15 Bohr magnetons; 2) for  $\text{CrMn}_6^*$  the product was amorphous and we never reached the saturation value of the magnetisation equal to the expected 27 Bohr magnetons. The synthetic route described in the present paper, initiated by Mallah in our group<sup>[31, 32]</sup> and then followed by others,<sup>[33–35]</sup> leads to the formation of crystallographically well-defined heptanuclear complexes.

The reaction of hexacyanometalate precursor  $[\text{M}(\text{CN})_6]^{3-}$  ( $M=\text{Cr}^{III}, \text{Co}^{III}$ ), a Lewis base, with an excess of Lewis acid, that is, a mononuclear complex formed by a paramagnetic metal ion chelated by a multidentate terminal ligand  $L_n$  leaving one easily accessible free coordination position only, allows the formation of the target heptanuclear species  $[\text{M}(\text{CN}-\text{M}'\text{L}_n)_6]^{9+}$  ( $M'=Cu^{II}, Ni^{II}, Mn^{II}$ ) (Figure 2) by formation of six  $\text{M}-\text{CN}-\text{M}'$  coordination bonds.

The choice of the cyanide as bridging ligand is directed by two considerations: 1) as far as the synthesis and structure are concerned, the cyanide ion presents a number of useful singularities: it is well known to bridge two transition metal atoms in an end-to-end fashion;<sup>[36–38]</sup> cyanide is a nonsymmetrical bridge, allowing it to bind selectively two different transition metals; the polycyanometalate precursors are stable and often inert building blocks, especially the hexacyanochromate complex,  $[\text{Cr}(\text{CN})_6]^{3-}$  used in the present study;<sup>[39]</sup> 2) as far as the magnetic properties are concerned the cyanide, itself diamagnetic, allows strong exchange coupling between the spin carriers,<sup>[40]</sup> and thanks to the quasi linear configuration of the  $\text{M}-\text{CN}-\text{M}'$  unit, it is possible to foresee the nature and to tune the value of the orbital interactions through the cyanide by choosing the metallic centres  $M$  and  $M'$  involved, and therefore the spin ground state of the molecules. In the heptanuclear complexes

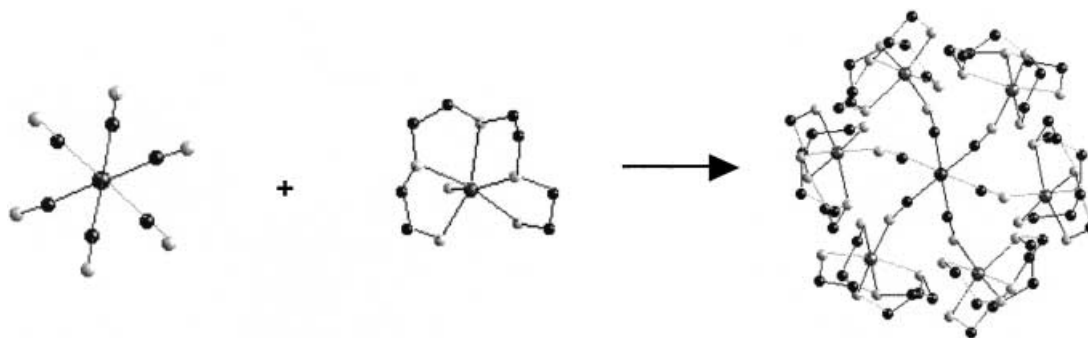


Figure 2. Synthetic strategy scheme.

$[\text{Cr}(\text{CN}-\text{M}'\text{L}_n)_6]^{9+}$ , whatever the nature of the interaction is (ferromagnetic or antiferromagnetic), high-spin values are foreseen and observed. In this radial symmetry, a short range ferromagnetic coupling between  $\text{M}$  and  $\text{M}'$  leads to a total spin ground state that is the sum of the spins:  $S_{\text{T}} = S_{\text{M}} + 6S_{\text{M}'}$ . A short-range antiferromagnetic coupling leads to a total spin ground state that is the difference between the spins:  $S_{\text{T}} = |S_{\text{M}} - 6S_{\text{M}'}|$ . To foresee the  $|J|$  value, the orbital models by Hoffmann et al. (orthogonalised magnetic orbitals)<sup>[41]</sup> or Kahn et al. (non-orthogonalised magnetic orbitals)<sup>[16, 42]</sup> are available. Both predict that orthogonal orbitals give rise to ferromagnetism (F) and that overlap can give rise to antiferromagnetism (AF). Such considerations determine the choice of the metallic ions.

The formation of highly charged cationic complexes is another key point of our synthetic strategy. The selection of a trivalent core ( $\text{M} = \text{Cr}^{\text{III}}$ ,  $d^3$ ,  $S = 3/2$ ;  $\text{Co}^{\text{III}}$ ,  $d^6$ ,  $S = 0$ ) and divalent peripheral metallic cations ( $\text{M}'$ ) together with neutral ligands ( $\text{L}$ ) avoids the precipitation of neutral products in aqueous solution and favours a slow growth of crystals. Furthermore, charged complexes allow the separation of the molecular ions in the solid state by various counter anions and a possible control of the intermolecular interactions. Another advantage of this strategy is the possible variations in several synthetic parameters such as the nature of the metallic cations, the polydentate ligands, the counter anions and the stoichiometry.

The peripheral transition metal ions that have been selected in the present study are copper(II) ( $d^9$ ), nickel(II) ( $d^8$ ) and manganese(II) ( $d^5$ ), chosen for their divalent charge state and their spin value,  $S = 1/2$ , 1 and  $5/2$ , respectively. A specific study also has been performed on a cobalt(II) precursor, leading to unexpected fascinating results that will be presented in a forthcoming publication.<sup>[43]</sup>

The selection of the terminal multidentate ligand  $\text{L}_n$  is determined by the ability of the ligand to leave only one free position accessible to the cyanide Lewis base. It must form stable and redox inactive  $\text{ML}_n$  mononuclear complexes in solution and present a steric configuration compatible with the formation of the heptanuclear species. We developed the synthesis of many polydentate amines, but two commercially available polyamine molecules proved to be the most useful and are utilised in the present study. Concerning the copper(II) compound, tris(2-amino)ethylamine (tren) has been used as a tetradentate ligand since it gives stable copper(II) complexes with a trigonal-bipyramidal geometry. Regarding the nickel(II)

and manganese(II) complexes, frequently encountered in an octahedral environment, the tetraethylenepentamine (tetren) ligand has been used, despite the fact that the ligand is known to adopt multiple conformations (up to eight).<sup>[44]</sup> The tetren ligand has never been adopted for manganese complexes, the chemistry of which is usually based on pentaazacyclopentadecane<sup>[45, 46]</sup> or polypyridine ligands.<sup>[32, 34, 47]</sup> In all cases the ligand plays the role of a blocking unit leaving one accessible position, as required by the synthetic strategy.

Despite their hazardous reactivity, perchlorate salts have been used because we were unable to get similar compounds with equivalent properties and good quality crystals with other counter anions, including tetrafluoroborate anions.

## Results and Discussion

**Synthesis:** All the heptanuclear complexes  $[\text{M}(\text{CN}-\text{M}'\text{L}_n)_6]^{9+}$  ( $\text{M} = \text{Cr}^{\text{III}}$ ,  $\text{Co}^{\text{III}}$ ,  $\text{M}' = \text{Cu}^{\text{II}}$ ,  $\text{Ni}^{\text{II}}$ ,  $\text{Mn}^{\text{II}}$ ,  $\text{L} = \text{tren}$  or  $\text{tetren}$ ) have been synthesised by the following method: the mononuclear species  $[\text{M}'\text{L}(\text{H}_2\text{O})]^{2+}$  is generated in situ by addition of the perchlorate salt of the desired metallic cation into an aqueous solution of the corresponding  $\text{L}_n$  ligand, before adding the stoichiometric amount of the hexacyanochromate(III) or hexacyanocobaltate(III) precursors.

The polynuclear complex  $[\text{M}(\text{CN}-\text{Cu}(\text{tren}))_6]^{9+}$  ( $\text{CrCu}_6$ ) was obtained by a dropwise addition of a potassium hexacyanochromate(III) solution to the mononuclear copper(II) complex generated in situ from the ligand tris(2-aminoethyl)amine (tren) and a  $\text{Cu}^{\text{II}}$  perchlorate salt. Partial evaporation of the solvent leads to hexagonal blue crystals. As discussed below, the X-ray diffraction structure reveals not only the presence of the expected heptanuclear compound but also of a "parasitic" co-crystallised trinuclear complex  $[\text{tren}\{\text{Cu}(\text{tren})\}_3]^{6+}$ . We checked the high stability of the trinuclear copper(II), already observed as a parasitic species in the literature.<sup>[48]</sup> Indeed, the trinuclear copper(II) species can be synthesised separately by another route and isolated as crystals. Many attempts to obtain good quality single crystals of the isolated  $\text{CrCu}_6$  complex (using all sorts of tetradentate ligands, counter anions, solvents and exchange-cation resins) failed, especially because of the appearance under the new synthetic conditions of  $\mu$ -cyano homodinuclear copper(II) complexes, other unwanted by-products of high thermodynamic stability which have been discussed previously.<sup>[39]</sup> Nevertheless, the pure isolated  $\text{CrCu}_6$  was obtained as a

powder or as very thin platelets similar to the ones obtained for the cobalt-centred analogue  $\text{CoCu}_6$ , and the characterizations of the product are in good agreement with the expected structure.

The polynuclear complexes  $[\text{M}\{\text{CN-Ni}(\text{tetren})\}_6]^{9+}$  ( $\text{CrNi}_6$ ) and  $[\text{M}\{\text{CN-Mn}(\text{tetren})\}_6]^{9+}$  ( $\text{CrMn}_6$ ) were obtained similarly using tetren as a blocking ligand and perchlorate salts. The purity of the ligand and the nature of the counter anions are of major importance. With respect to the  $\text{CrNi}_6$  complex, for example, when using the commercially available tetren, which contains several isomers, the quality of the crystals is not good enough to allow a full determination of the crystallographic structure. Under such conditions, preliminary results indicate the formation of the  $\text{CrNi}_6^*$  product with disorder on the terminal polyamine ligand.<sup>[31]</sup> By using the tetren hydrochloride salt, commercially available at a suitable purity level, the final product is not the target heptanuclear product but a chloride salt of a trinuclear  $\text{CrNi}_2$  complex,  $[\text{Cr}(\text{CN})_4\{\text{CN-Ni}(\text{tetren})\}_2]\text{Cl}$ .<sup>[49]</sup> To selectively obtain the pure  $\text{CrNi}_6$ , it is necessary to avoid the presence of chloride ions. For this purpose, tetren hydrochloride salt has been used for the synthesis in situ of the mononuclear complex and the chloride was exchanged with perchlorate by addition of silver perchlorate salt and filtration of  $\text{AgCl}$  precipitate before adding the hexacyanochromate solution. The recrystallisation in the presence of sodium perchlorate salt gives octahedral red crystals of the target  $\text{CrNi}_6$  product.

A similar procedure has been used for the chromium–manganese heptanuclear complex  $\text{CrMn}_6$ . The reaction was performed under an argon atmosphere to avoid the formation of parasitic  $\mu$ -oxo dinuclear manganese(III) complexes.<sup>[50]</sup> The final  $\text{CrMn}_6$  product obtained as large brown crystals is slightly sensitive to oxygen. Due to the nature of the pentadentate ligand (tetren), this  $\text{CrMn}_6$  heptanuclear complex is different from the amorphous one based on the manganese trispicmeen precursor,<sup>[32]</sup> and from that recently described by Murray and co-workers.<sup>[34]</sup>

To evaluate exchange interactions between external metallic cations, similar polynuclear complexes with diamagnetic cobalt(III) cores have been obtained by using hexacyanocobaltate(III) as precursor. Following a similar synthetic strategy,  $\text{CoCu}_6$ ,  $\text{CoNi}_6$  and  $\text{CoMn}_6$  heptanuclear complexes have been synthesised and fully characterised.

The  $\text{CoCu}_6$  synthesis leads to two different types of crystals in the same reaction medium: a minor fraction of crystals is isostructural with the  $\text{CrCu}_6$  (B form) analogue with the trinuclear copper(II) side product and the other fraction is made of pure  $\text{CoCu}_6$  without trinuclear copper(II) species (A form). The  $\text{CoMn}_6$  complex, which grows as light yellow crystals, is isostructural with the chromium  $\text{CrMn}_6$  analogue. With respect to the nickel species, two different results have been obtained: 1) Addition of the hexacyanocobaltate precursor to a nickel perchlorate salt as starting material in the presence of pure tetren gave a hexanuclear complex  $\text{CoNi}_5$  will be described in detail in Part 2.<sup>[18]</sup> 2) Starting with tetren and a mixture of chloride and perchlorate nickel salts, led to the formation of  $\text{CoNi}_6$ , which has been isolated as crystals of defective quality, the characterizations of which are in agreement with the expected structure.

The synthetic strategy used in the present study allows us not only to synthesise well known heptanuclear clusters, but also to define the experimental and the recrystallisation conditions of the chemical reaction that might thus be extended to other polycyanometalate precursors.

**Infrared spectroscopy:** The heptanuclear complexes  $\text{CrCu}_6$ ,  $\text{CrNi}_6$ ,  $\text{CrMn}_6$ ,  $\text{CoCu}_6$ ,  $\text{CoNi}_6$  and  $\text{CoMn}_6$  have been characterised by their infrared spectra. In all cases, the intense distinctive broad band of the perchlorate anion (around  $1090\text{ cm}^{-1}$ ) clearly indicates the presence of charged cationic complexes. In the frequency range of the stretching of the cyanide,  $2200\text{--}2000\text{ cm}^{-1}$ , a unique CN asymmetric stretching band is observed: for the hexacyanochromate(III) derivatives,  $\text{CrCu}_6$  exhibits a weak band at  $2180$ ,  $\text{CrNi}_6$  at  $2149$  and  $\text{CrMn}_6$  at  $2146\text{ cm}^{-1}$ ; for the hexacyanocobaltate(III) derivatives,  $\text{CoCu}_6$  presents a band at  $2188$ ,  $\text{CoNi}_6$  at  $2152$  and  $\text{CoMn}_6$  at  $2129\text{ cm}^{-1}$  ( $2137\text{ cm}^{-1}$  sh). For comparison, the corresponding values for the cyanide of the tripotassium hexacyanochromate(III) and hexacyanocobaltate(III) complexes are  $2131$  and  $2130\text{ cm}^{-1}$ , respectively.<sup>[51]</sup> Considering that the CN bridging group usually absorbs at a higher frequency than the terminal group, it appears that the stretching  $\nu_{\text{CN}}$  bands for all the heptanuclear complexes are characteristic of bridging cyano groups. To analyse these results, the simplest discussion might be based on the electronegativity of the metallic ions involved in the polynuclear structures, according to El-Sayer and Sheline.<sup>[51]</sup> In such a hypothesis (the lower the electronegativity, the lower the frequency), since the value of the electronegativity of the metals increases in the order  $\text{Mn} < \text{Ni} < \text{Cu}$ , the CN stretching frequency of the  $\text{CrMn}_6$  complex has to be the lowest in the series  $\text{CrMn}_6 < \text{CrNi}_6 < \text{CrCu}_6$  and  $\text{CoMn}_6 < \text{CoNi}_6 < \text{CoCu}_6$  as observed experimentally.

Orbital considerations might also be used for the interpretation of the infrared spectra. Although the description of the bonding is more complex, the concept of the  $\sigma$  basicity and  $\pi$  acidity also remains useful for interpreting the influence of metal–ligand  $\pi$  bonding on the CN stretching band in polycyanometalate complexes. An electron-poor metal centre that has d orbitals lowered in energy induces a shorter CN bond and a higher CN stretching frequency. An electron-rich centre generates a highly populated CN  $\pi$ -antibonding orbital, so that the CN bond is weakened. As a result, the CN bond lengthens slightly and the CN stretching frequency decreases.

Considering copper(II) metallic ions, for instance, the absence of back donation between  $\text{Cu}^{\text{II}}$  and the  $\pi^*$  orbital might explain the high  $\nu_{\text{CN}}$  value observed for the  $\text{CrCu}_6$  complexes at  $2180\text{ cm}^{-1}$  and we can therefore expect a quasi-linear  $\text{Cr-CN-Cu}$  bond. On the other hand, the electronic configuration of the  $\text{Mn}^{\text{II}}$  complexes and the predicted electron delocalisation might explain the CN stretching frequencies observed for the  $\text{CrMn}_6$  complexes at  $2146\text{ cm}^{-1}$ . The distortion of the cyano bridge, induced by the populated CN  $\pi$ -antibonding orbital and directly correlated to the stretching frequency, is discussed further through the crystallographic X-ray structure and the magnetostructural correlation.

**Crystallographic structures:** The heptanuclear compounds CrCu<sub>6</sub>, CrNi<sub>6</sub>, CrMn<sub>6</sub>, CoCu<sub>6</sub> and CoMn<sub>6</sub> have been characterised by single-crystal X-ray diffraction. The crystallographic data and the details of the refinements have been deposited at the Cambridge Crystallographic Data Centre and are reported in a condensed form in Table 1. The key distances and angles are reported in Table 2. In all cases, the heptanuclear entity [M(CN–ML)<sub>6</sub>]<sup>9+</sup> is well defined, without disorder on the polyamine ligand and with a unique conformation for the tetren ligand. The crystal system (trigonal) and the space group (*R* $\bar{3}$ ) obtained for all the compounds demonstrate the high symmetry of the molecular and crystal structures.

The cell parameters for crystals of the CrCu<sub>6</sub> complex (B form) are very peculiar, especially the *c* value (*a* = *b* = 15.169(5) and *c* = 77.305(17) Å, *V* = 15 398(12) Å<sup>3</sup>). In addition to the expected heptanuclear complex CrCu<sub>6</sub>, a trinuclear entity, [tren{Cu(tren)}<sub>3</sub>]<sup>6+</sup> (Cu<sub>3</sub>) is present in the unit cell, with a CrCu<sub>6</sub>/Cu<sub>3</sub> ratio of 1:2 (Figure 3). This trinuclear complex is formed with by [Cu(tren)]<sup>2+</sup> mononuclear fragments linked together by a residual tren ligand (Figure 4).

Along the *b* axis, layers of [Cr{CN–Cu(tren)}<sub>6</sub>]<sup>9+</sup> entities are separated by the [tren{Cu(tren)}<sub>3</sub>]<sup>6+</sup> species with an average distance of 27.6 Å between two layers. The electro-neutrality is ensured by the presence of 21 perchlorate anions to compensate the nine positive charges of the [Cr{CN–Cu(tren)}<sub>6</sub>]<sup>9+</sup> complex and the six charges of each of the two trinuclear compounds. The [Cr{CN–Cu(tren)}<sub>6</sub>]<sup>9+</sup> entity is formed by the hexacyanochromate core, with the chromium center in an octahedral environment and six copper(II) ions fixed on the six available nitrogen atoms. The

copper atoms are in a trigonal-bipyramid geometry, in which the tren ligand plays the role of blocking ligand. The cyano bridge appears quasi-linear with Cr–C–N and C–N–Cu angles of 176.4(9) and 176.5(9)°, respectively. A more complete structural description will be carried out as a comparative discussion between the whole complexes.

When the experimental conditions were changed slightly, the CrCu<sub>6</sub> complex was obtained as thin platelets, the quality of which was not sufficient to allow the determination of the X-ray structure. Nevertheless, this compound can be considered as the heptanuclear complex without co-crystallised trimers (A form). The nature of the product is further substantiated by the two X-ray crystallographic structures of the CoCu<sub>6</sub> complex, solved with and without the parasitic trimers (B and A forms, respectively).

The structure of CoCu<sub>6</sub> (B form) is isostructural with that obtained for the CrCu<sub>6</sub> complex. The crystallographic structure of CoCu<sub>6</sub> (A form) indicates that only the heptanuclear entity [Co{CN–Cu(tren)}<sub>6</sub>]<sup>9+</sup> is present in the unit cell, with the nine expected perchlorate ions, water and acetonitrile molecules. As in CrCu<sub>6</sub> (B) the copper atom is in a trigonal-bipyramid geometry, the cobalt atom is in an octahedral environment and the cyano bridge is close to linearity with Co–C–N and C–N–Cu angles of 178.7(18)° and 175.7(12)°, respectively.

Despite the number of similarities between CrNi<sub>6</sub> and CrMn<sub>6</sub>, both complexes being prepared using the tetren ligand and perchlorate salts, the two crystals are not isostructural.

The unit cell parameters for CrNi<sub>6</sub> (Figure 5) are *a* = *b* = 15.274(4) and *c* = 41.549(7) Å in a trigonal system. They differ

Table 1. Crystallographic data of the heptanuclear complexes: CrCu<sub>6</sub>, CrNi<sub>6</sub>, CrMn<sub>6</sub>, CoCu<sub>6</sub> and CoMn<sub>6</sub>.

	CrCu <sub>6</sub> [Cr{CNCu(tren)} <sub>6</sub> ], [tren{Cu(tren)} <sub>3</sub> ] <sub>2</sub> , (ClO <sub>4</sub> ) <sub>21</sub>	CrNi <sub>6</sub> [Cr{CNNi(tetren)} <sub>6</sub> ], (ClO <sub>4</sub> ) <sub>9</sub> (H <sub>2</sub> O) <sub>2</sub>	CrMn <sub>6</sub> [Cr{CNMn(tetren)} <sub>6</sub> ] <sub>2</sub> , [Mn(tetren)(H <sub>2</sub> O)] <sub>2</sub> (ClO <sub>4</sub> ) <sub>22</sub>	CoCu <sub>6</sub> [Cr{CNCu(tren)} <sub>6</sub> ], (ClO <sub>4</sub> ) <sub>9</sub> (CH <sub>3</sub> CN) <sub>2</sub> (H <sub>2</sub> O) <sub>3</sub>	CoMn <sub>6</sub> [Co{CNMn(tetren)} <sub>6</sub> ] <sub>2</sub> , [Mn(tetren)(H <sub>2</sub> O)] <sub>2</sub> - (ClO <sub>4</sub> ) <sub>22</sub>	Cu <sub>3</sub> [tren{Cu(tren)} <sub>3</sub> ]- (ClO <sub>4</sub> ) <sub>6</sub>
chemical formula	CrCu <sub>12</sub> C <sub>90</sub> H <sub>252</sub> - N <sub>62</sub> Cl <sub>21</sub> O <sub>84</sub>	CrNi <sub>6</sub> C <sub>34</sub> H <sub>150</sub> - N <sub>36</sub> Cl <sub>9</sub> O <sub>38</sub>	Cr <sub>2</sub> Mn <sub>14</sub> C <sub>124</sub> H <sub>326</sub> - N <sub>82</sub> Cl <sub>22</sub> O <sub>90</sub>	CoCu <sub>6</sub> C <sub>35</sub> H <sub>120</sub> - N <sub>30</sub> Cl <sub>9</sub> O <sub>39</sub>	Co <sub>2</sub> Mn <sub>14</sub> C <sub>124</sub> H <sub>326</sub> - N <sub>82</sub> Cl <sub>22</sub> O <sub>90</sub>	C <sub>24</sub> H <sub>72</sub> N <sub>16</sub> Cu <sub>3</sub> - Cl <sub>6</sub> O <sub>24</sub>
Fw	5106.44	2635.29	6059.56	2504.90	6073.28	1372.29
crystal system	trigonal	trigonal	trigonal	trigonal	23	monoclinic
<i>a</i> [Å]	15.169(5)	15.274(7)	23.288(18)	15.051(7)	23.267(7)	16.259(3)
<i>b</i> [Å]	15.169(5)	15.274(7)	23.288(11)	15.051(7)	23.267(9)	17.291(2)
<i>c</i> [Å]	77.305(17)	41.549(7)	40.644(23)	41.076(24)	40.478(17)	19.996(3)
$\alpha$ [°]	90	90	90	90	90	90
$\beta$ [°]	90	90	90	120	90	104.92 (1)
$\gamma$ [°]	120	120	120	90	120	90
<i>V</i> [Å <sup>3</sup> ]	15 398(12)	8395(4)	19 094(23)	8047(8)	19 094(23)	5432(1)
<i>Z</i>	3	3	6	3	6	4
space group	<i>R</i> $\bar{3}$	<i>R</i> $\bar{3}$	<i>R</i> $\bar{3}$	<i>R</i> $\bar{3}$	<i>R</i> $\bar{3}$	<i>P</i> 2 <sub>1</sub> / <i>a</i>
crystal shape	hexagonal plates	octahedral	parallelepiped	parallelepiped	parallelepiped	parallelepiped
crystal color	blue	red	orange-brown	blue	pale yellow	blue
data collected	6759	4985	8067	3506	8015	10 382
unique data collected	6010	4489	7466	3081	7417	9546
data used for refinement (( <i>F</i> <sub>o</sub> ) <sup>2</sup> > 3σ( <i>F</i> <sub>o</sub> ) <sup>2</sup> )	3071	2642	2262	1477	2248	4225
<i>R</i> <sup>[a]</sup>	0.0786	0.0881	0.141	0.1007	0.129	0.0473
<i>R</i> <sub>w</sub> <sup>[b]</sup>	0.0928	0.0951	0.154	0.1192	0.144	0.0565
variables	416	178	229	182	229	659
$\Delta\rho_{\min}$ [e Å <sup>-3</sup> ]	-0.90	-1.73	-0.78	-1.04	-1.34	-0.49
$\Delta\rho_{\max}$ [e Å <sup>-3</sup> ]	1.20	3.69	1.45	0.73	1.14	0.76

[a]  $R = \sum ||F_o| - |F_c|| / \sum |F_o|$ . [b]  $R_w = [\sum w(|F_o| - |F_c|)^2 / \sum w F_o^2]^{1/2}$ .

Table 2. Selected bond lengths [Å] and angles [°] in the complexes CrCu<sub>6</sub>, CrNi<sub>6</sub>, CrMn<sub>6</sub>, CoCu<sub>6</sub> and CoMn<sub>6</sub>.

	CrCu <sub>6</sub>	CrNi <sub>6</sub>	CrMn <sub>6</sub> <sup>[a]</sup>		CoCu <sub>6</sub>	CoMn <sub>6</sub> <sup>[a]</sup>	
interatomic distances [Å]			Mn1	Mn2		Mn1	Mn2
C–N bridge	1.14(1)	1.154(9)	1.12	1.12	1.178(17)	1.15	1.11
Cr (or Co)–cyanide	1.996(8)	2.077(6)	2.06	2.05	1.861(14)	1.91	1.87
M–cyanide	1.97(1)	2.113(6)	2.21	2.24	1.928(13)	2.16	2.31
M–N11	2.10(2)	2.130(6)	2.26	2.26	2.019(12)	2.26	2.24
M–N12	2.045(9)	2.081(7)	2.30	2.30	2.036(13)	2.28	2.35
M–N13	2.019(9)	2.133(6)	2.32	2.34	2.107(13)	2.31	2.29
M–N14	2.09(1)	2.117(6)	2.27	2.33	2.066(14)	2.26	2.37
M–N15	–	2.084(6)	2.30	2.34	–	2.30	2.30
bond angles [°]							
Cr (or Co)–C1–N1 cyanide	176.4(9)	174.6(6)	173.8	175.7	178.7(12)	176.0	179.3
C1–N1–M cyanide	176.5(9)	164.6(6)	161.7	153.6	175.7(12)	166.6	145.7
N11–M–cyanide	98.3(5)	91.2(3)	88.6	91.4	177.7(6)	90.8	92.5
N12–M–cyanide	94.8(4)	91.3(3)	151.9	160.6	93.8(5)	150.7	161.6
N13–M–cyanide	177.6(4)	89.8(3)	88.4	88.4	96.8(6)	86.5	87.7
N14–M–cyanide	93.8(4)	169.2(3)	93.3	94.3	95.1(6)	91.2	93.8
N15–M–cyanide	–	90.3(3)	105.2	100.2	–	110.3	101.0
N11–M–N12	118.1(5)	81.4(3)	76.7	78.1	84.2(6)	76.5	76.0
N11–M–N13	84.0(4)	162.7(3)	114.9	107.9	85.2(6)	116.8	108.9
N11–M–N14	115.9(6)	97.6(3)	169.5	173.1	85.1(6)	168.3	172.9
N11–M–N15	–	96.7(3)	94.4	97.8	–	92.5	98.0
N12–M–N13	84.7(4)	81.3(3)	76.7	79.6	118.7(7)	76.3	82.7
N12–M–N14	123.1(5)	96.3(3)	105.6	97.3	123.9(7)	106.5	93.8
N12–M–N15	–	177.5(3)	99.8	97.3	–	96.7	94.8
N13–M–N14	84.5(4)	83.7(3)	75.5	76.1	114.9(7)	74.9	74.5
N13–M–N15	–	100.6(3)	148.2	152.7	–	146.5	151.1
N14–M–N15	–	82.4(3)	75.1	77.4	–	76.0	77.7

[a] Due the poor quality of the X-ray structure, only approximate values are given.

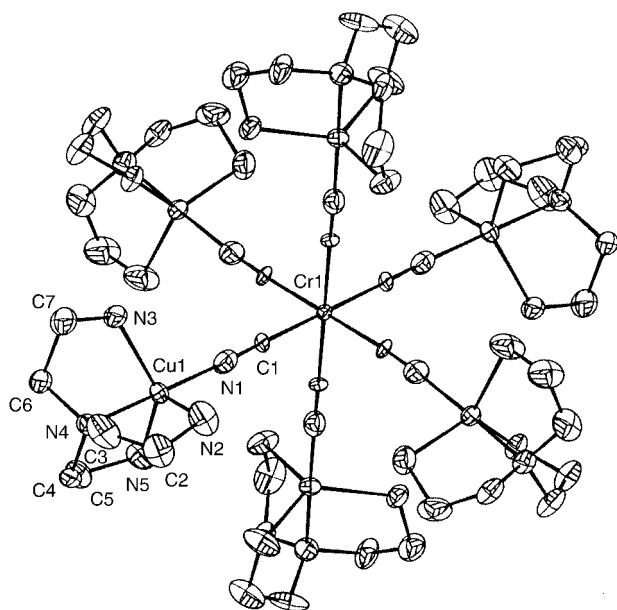


Figure 3. X-ray crystal structure of the  $[\text{Cr}\{\text{CN-Cu}(\text{tren})\}_6]^{9+}$  entity in  $\text{CrCu}_6$ .

from the ones already published.<sup>[31]</sup> Two heavy atoms only are present in the asymmetric unit: the chromium atom located at the origin of the unit cell on an inversion centre and the nickel atom in a general position. The nickel ion is in an octahedral symmetry, surrounded by six nitrogen atoms, including those of the pentaamine ligand. A distorted cyano bridge links the two metallic atoms (Cr–C–N and C–N–Ni angles are 174.6(6) and 164.6(6)°, respectively). The operation around the  $-3$

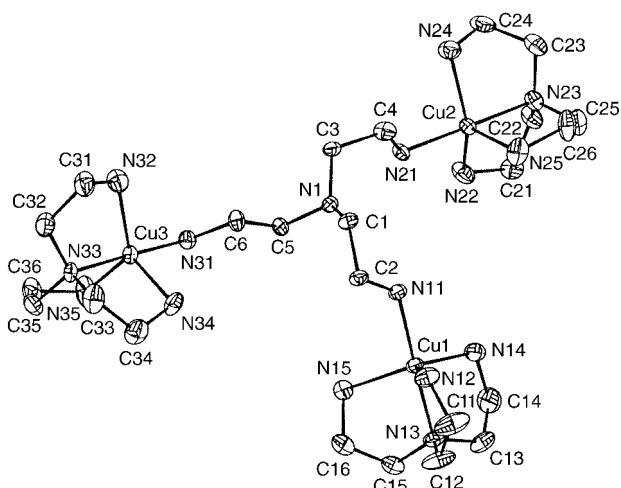


Figure 4. X-ray crystal structure of the  $[\text{tren}\{\text{Cu}(\text{tren})\}_3]^{6+}$  entity in  $\text{Cu}_3$ .

axis generates the heptanuclear complex. Three  $[\text{Cr}\{\text{CN-Ni}(\text{tetren})\}_6]^{9+}$  entities are present in the unit cell, related to each other by inversion symmetry and rotation around a three-fold screw axis along the  $c$  axis. As expected for the charge balance, eighteen perchlorate anions are found in the unit cell.

The  $\text{CrMn}_6$  crystallographic structure is more complex and sufficient data were not available to perform the refinement with anisotropic thermal parameters. The structure displays the presence of two crystallographically independent heptanuclear  $[\text{Cr}\{\text{CN-Mn}(\text{tetren})\}_6]^{9+}$  entities and of a mononuclear complex  $[\text{Mn}(\text{tetren})(\text{H}_2\text{O})]^{2+}$ . The asymmetric unit contains five heavy atoms, four of which generate the two

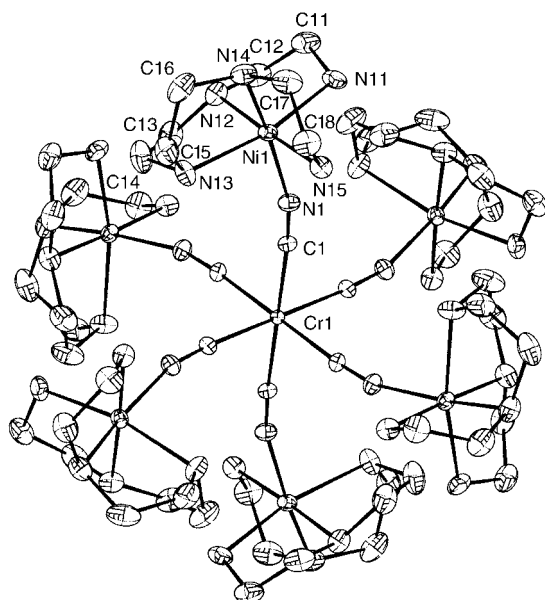


Figure 5. X-ray crystal structure of the  $[\text{Cr}\{\text{CN-Ni}(\text{tetren})\}]_6^{9+}$  entity in  $\text{CrNi}_6$ .

heptanuclear entities by a  $-3$  axis and an inversion centre as in the  $\text{CrNi}_6$  complex; the last transition metal is associated with the presence of the crystallographically disordered mononuclear complex  $[\text{Mn}(\text{tetren})(\text{H}_2\text{O})]^{2+}$ . The overall configuration of the two  $[\text{Cr}\{\text{CN-Mn}(\text{tetren})\}]_6^{9+}$  units is the same but they differ from each other by the distortion of the cyano bridge between Cr and Mn: in one unit the Mn-N-C angle is about  $155.2^\circ$ , whereas it is  $161.7^\circ$  in the other (Figure 6). The volume of the unit cell, filled with six heptanuclear compounds, six mononuclear complexes, and sixty-six perchlorate ions reaches the remarkable value of  $19094 \text{ \AA}^3$ . Beside the interest of the  $\text{CrMn}_6$  compound itself, the present structure displays the first example of a “ $\text{Mn}^{\text{II}}(\text{tetren})$ ” entity identified by X-ray crystallography (Figure 7).

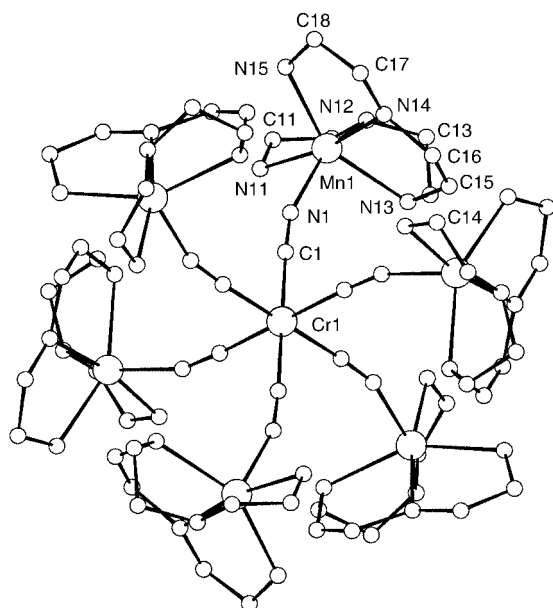


Figure 6. X-ray crystal structure of one of the two  $[\text{Cr}\{\text{CN-Mn}(\text{tetren})\}]_6^{9+}$  entities in  $\text{CrMn}_6$ .

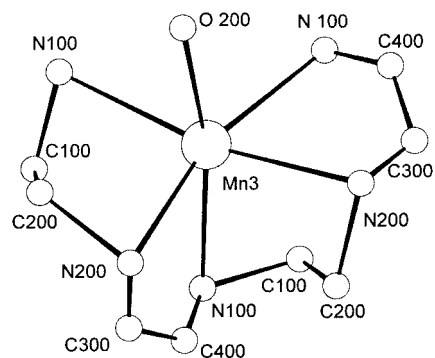


Figure 7. X-ray crystal structure of the mononuclear  $[\text{Mn}(\text{tetren})(\text{H}_2\text{O})]^{2+}$  ion in  $\text{CrMn}_6$ .

It clearly demonstrates the stability of this N-bonded manganese complex.

The selected metric data of the five molecular entities  $\text{CrCu}_6$ ,  $\text{CrNi}_6$ ,  $\text{CrMn}_6$ ,  $\text{CoCu}_6$  and  $\text{CoMn}_6$  are compiled in Table 2 for a comparative structural study. The C–N bond lengths are similar in the five structures:  $1.14(1)$  ( $\text{CrCu}_6$ ),  $1.154(9)$  ( $\text{CrNi}_6$ ),  $1.14(2)$  and  $1.11(2)$  ( $\text{CrMn}_6$ ),  $1.178(17)$  ( $\text{CoCu}_6$ ),  $1.15(2)$  and  $1.11(2)$   $\text{\AA}$  ( $\text{CoMn}_6$ ). The Cr–C bond length is notably short at  $1.996(8)$   $\text{\AA}$  in the case of the  $\text{CrCu}_6$  complex, whereas it remains in the range  $2.06(\pm 0.02)$  in the two other compounds ( $2.077(6)$ ,  $\text{CrNi}_6$ ;  $2.08(2)$  and  $2.051(19)$   $\text{\AA}$ ,  $\text{CrMn}_6$ ), as expected for hexacyanochromate species. In the hexacyanocobaltate(III) complexes the Co–C distances are shorter,  $1.861(14)$  ( $\text{CoCu}_6$ ),  $1.91(2)$  and  $1.866(18)$   $\text{\AA}$  ( $\text{CoMn}_6$ ), in agreement with similar cobaltocyanide cores.<sup>[53]</sup> The main differences observed deal with the distortion of the M–CN–M' bridge and especially the C–N–M' angle varying from  $176.5(9)^\circ$  for  $\text{CrCu}_6$  to  $155.2(16)$  for one of the  $\text{CrMn}_6$  entities.

This difference might be explained by the electronic configuration of the external cation, M', and principally the  $t_{2g}/e_g$  orbitals more or less involved in back donation with the empty CN  $\pi$ -antibonding orbital as discussed previously. According to the electronic configurations of the external ions M' ( $t_{2g}$  and  $e_g$  symmetry), different situations may occur: with  $\text{M} = \text{Cu}^{\text{II}}$  ( $d_{z^2}$  orbital,  $e_g$  local symmetry) and to a lesser extent with  $\text{Ni}^{\text{II}}$  (also with  $e_g$  electrons), there is no back donation. However, with the  $\text{Mn}^{\text{II}}$  complexes, an effective back donation is expected. These considerations are in agreement with the importance of the distortion: minimal for  $\text{CrCu}_6$  and at the maximum for the  $\text{CrMn}_6$  complex, the  $\text{CrNi}_6$  species being in between. This is consistent with the binding model because an increase in the electronic density on the metal atom is delocalised over the CN ligand thereby weakening the CN bond by populating the cyano  $\pi^*$  orbital. Another illustration of the effect is the decrease in stretching frequency observed in the infrared spectra when electronegativity decreases.

**Mass spectrometry:** To characterise the polynuclear complexes and to evaluate their thermodynamic stability in solution, mass spectrometry has been performed for all the heptanuclear species. Electrospray desorption–ionisation was used to characterise these highly charged complexes. The best-resolved spectrum was obtained for  $\text{CrCu}_6$ ,



with a major peak at  $m/z$  1080 assigned to  $\{[\text{Cr}(\text{CN}-\text{CuL})_6](\text{ClO}_4)_7\}^{2+}$ , denoted as  $\{[\text{CrCu}_6](\text{ClO}_4)_7\}^{2+}$  (Figure 8).

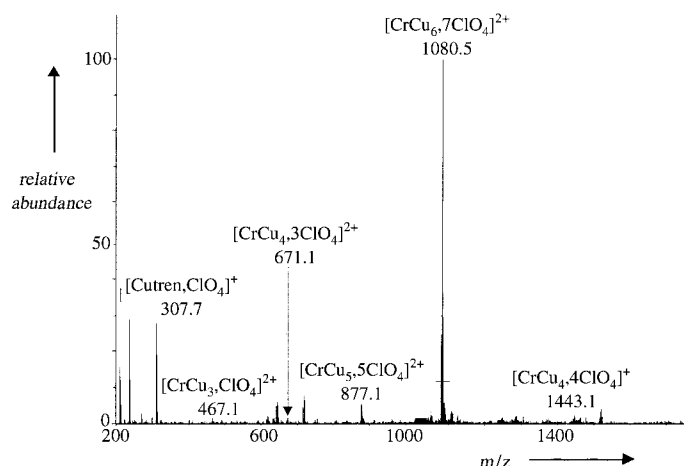


Figure 8. Mass spectrum of  $\text{CrCu}_6$ .

With the high energetic parameters induced by a high difference potential (180 V) between the capillary exit and the skimmer, other peaks appear on the spectrum at  $m/z = 493$ , 293 and 236 assigned to  $\{[\text{CrCu}_6](\text{ClO}_4)_5\}^{4+}$ ,  $\{[\text{CrCu}_6](\text{ClO}_4)_3\}^{6+}$  and  $\{[\text{CrCu}_6](\text{ClO}_4)_2\}^{7+}$ , respectively. The peaks of the trinuclear copper(II) complex are observed at  $m/z$  1271 and 584 corresponding to  $\{[\text{tren}(\text{Cutren})_3](\text{ClO}_4)_5\}^+$  and  $\{[\text{tren}(\text{Cutren})_3](\text{ClO}_4)_4\}^{2+}$ . The spectrum also displays peaks of the hexa  $\{[\text{CrCu}_5](\text{ClO}_4)_5\}^{2+}$ , penta  $\{[\text{CrCu}_4](\text{ClO}_4)_3\}^{2+}$ , and tetra  $\{[\text{CrCu}_3](\text{ClO}_4)_2\}^{2+}$  nuclear species as doubly charged cations (at  $m/z$  877, 671 and 467). The distribution of the corresponding peaks is a distorted Gaussian curve with a maximum for the tetranuclear complex. This distribution is a clear indication that these species are fragmentation products induced by the mass technique.

Similar results obtained for the  $\text{CrNi}_6$  and  $\text{CrMn}_6$  complexes are collected in Table 3. Most of the observed peaks correspond to doubly charged cations: the peaks correspond-

Table 3. Observed peaks and corresponding species detected by mass spectrometry for  $\text{CrCu}_6$ ,  $\text{CrNi}_6$ ,  $\text{CrMn}_6$ ,  $\text{CoCu}_6$ ,  $\text{CoNi}_6$  and  $\text{CoMn}_6$ .

Observed peaks: $m/z$	Observed peaks: $m/z$	Attribution (M = Co or Cr)
$\text{CrCu}_6$	$\text{CoCu}_6$	
1080	1084	$\{[\text{MCu}_6](\text{ClO}_4)_7\}^{2+}$
493	495	$\{[\text{MCu}_6](\text{ClO}_4)_5\}^{4+}$
293	294	$\{[\text{MCu}_6](\text{ClO}_4)_3\}^{6+}$
236	236	$\{[\text{MCu}_6](\text{ClO}_4)_2\}^{7+}$
877	881	$\{[\text{MCu}_5](\text{ClO}_4)_5\}^{2+}$
671	674	$\{[\text{MCu}_4](\text{ClO}_4)_3\}^{2+}$
467	471	$\{[\text{MCu}_3](\text{ClO}_4)_2\}^{2+}$
$\text{CrNi}_6$	$\text{CoNi}_6$	
1194	1199	$\{[\text{MNi}_6](\text{ClO}_4)_7\}^{2+}$
972	975	$\{[\text{MNi}_5](\text{ClO}_4)_5\}^{2+}$
1596	1601	$\{[\text{MNi}_4](\text{ClO}_4)_3\}^{2+}$
747	751	$\{[\text{MNi}_3](\text{ClO}_4)_2\}^{2+}$
1151	1155	$\{[\text{MNi}_3](\text{ClO}_4)_4\}^+$
$\text{CrMn}_6$	$\text{CoMn}_6$	
1185	1188	$\{[\text{MMn}_6](\text{ClO}_4)_7\}^{2+}$
967	971	$\{[\text{MMn}_5](\text{ClO}_4)_5\}^{2+}$
742	746	$\{[\text{MMn}_4](\text{ClO}_4)_3\}^{2+}$
1138	1145	$\{[\text{MMn}_3](\text{ClO}_4)_2\}^{2+}$

ing to the monocations  $\{[\text{CrM}_6](\text{ClO}_4)_8\}^+$  are not visible because they are outside the observation range. We interpret the absence of peaks belonging to the higher charged states ( $[\text{CrM}_m]^{3+}$ ,<sup>[4–8]</sup> with  $m = 2–6$ ) by the high stability of the heptanuclear entity strongly associated with the counter anions. This special stability was checked by using high energy parameters. No significant changes in the mass spectra occurred, demonstrating that the ejection of the perchlorate anion from the “external coordination sphere” of the complex is difficult. In all cases, the distorted Gaussian distribution of the doubly charged ion peaks is observed. Despite the relative complexity of the spectrum and by analogy with the spectra of other complexes, the results indicate the presence and the stability of the heptanuclear complexes in methanol/acetonitrile solution.

Concerning the  $\text{CrMn}_6$  and  $\text{CoMn}_6$  complexes, a priori more sensitive products, the relative stability of the compounds in solution is quite remarkable in an anaerobic medium. However the stability decreases rapidly in aerobic solution.

**Magnetic studies:** Magnetisation measurements have been performed on all the heptanuclear complexes with a SQUID magnetometer in the temperature range of  $T = 2–300$  K in an applied field  $H = 200$  Oe and at  $T = 2$  K in an applied field range  $H = 0–5 \times 10^4$  Oe. We discuss in the following the results of the chromium(III) derivatives ( $\text{CrCu}_6$ ,  $\text{CrNi}_6$  and  $\text{CrMn}_6$ ) and then those obtained for the cobalt(II)-centred compounds ( $\text{CoCu}_6$ ,  $\text{CoNi}_6$  and  $\text{CoMn}_6$ ).

The analysis of the magnetisation of the chromium(III) derivatives is relatively simple because: i) in a  $\text{CrM}_6$  entity there is one central paramagnetic centre surrounded by six identical other centres, leading to a unique  $J$  value between chromium and its first neighbours; ii) the peripheral paramagnetic centres are far from each other (more than  $10 \text{ \AA}$  through the chromium centre) and in a first approximation, the exchange coupling constant  $J_{nn}$  (next nearest neighbours) can be neglected; iii) the intermolecular interaction  $zJ'$  ( $z =$  number of magnetic neighbouring units) is expected to be weak, due to the insulating role of the counter-anions; iv) the octahedral symmetry of the hexanuclear units precludes the presence of a significant  $D$  factor in the ground state and can be ignored; v) in this way a simple analytical expression of the molar susceptibility  $\chi_M$  becomes available through the solutions of the isotropic Heisenberg Hamiltonian ( $i$  ranges from 1 to 6; [Eq. (1)].<sup>[54]</sup>

$$\mathcal{H} = -J_{\text{CrI}} S_{\text{Cr}} \cdot \sum_i S_i \quad (1)$$

The energy spin state diagrams  $E(S)/J = f(S)$  for the three entities  $[\text{Cr}(\text{CN}-\text{M})_6]^{9+}$  ( $\text{M} = \text{Cu}, \text{Ni}, \text{Mn}$ ) are shown in Table S1 in the Supporting Information. They display the remarkable energy/spin structure for two ferromagnetic high spin complexes (where the highest spin is at the ground state) and the ferrimagnetic one (where the highest spin lies at the highest energy). The diagram, first used to the best of our knowledge in reference [55] also demonstrates the original nature of such high-spin complexes, with the coexistence of

discrete quantum levels and a quasi continuum of energy levels, in between quantum and classical physics.

The thermal variation of the magnetisation allows us to determine the nature and magnitude of the exchange intramolecular interaction, the exchange coupling constant  $J$  and the Lande factor  $g$ . The best-fit values are given in Table 4. To take into account the decrease of  $\chi_M$  at low temperature, we included either a weak intermolecular interaction  $zJ'$  (using a mean field approach:  $(\chi_M)_{\text{cor}} = (\chi_M)_{\text{cal}} [T/T - \theta]$ ) or zero field splitting  $D$  of the ground state. The new Hamiltonian is then given by Equation (2) with  $D$  the uniaxial anisotropy and  $E$  the rhombic one.

$$\mathcal{H} = \frac{J}{2}(\hat{S}_z^2 - \hat{S}_M^2 - \hat{S}_{M'}^2) + D(\hat{S}_z^2 - \frac{\hat{S}_z^2}{3}) + E(\hat{S}_x^2 - \hat{S}_y^2) \quad (2)$$

The high symmetry of the heptanuclear complexes implies that  $D$  and  $E$  are very small. For the fits, in the first approximation,  $E$  is chosen equal to zero and  $D$  is the only anisotropic parameter involved. The agreement factor  $R$  for the fits is defined as  $R = \frac{\sum_i [(\chi_M)_{\text{obs}}(i) - (\chi_M)_{\text{calcd}}(i)]^2}{\sum_i [(\chi_M)_{\text{obs}}(i)]^2}$ .

The magnetisation as a function of the magnetic field at low temperature ( $T=2$  K) allows a direct determination of the ground spin state when the saturation value  $gS$  is reached at high field ( $H=5 \times 10^4$  Oe in the present case) and can be compared to the theoretical Brillouin function.

**Magnetic properties of CrCu<sub>6</sub>:** Two different samples of CrCu<sub>6</sub> are available: CrCu<sub>6</sub>-A, without parasitic trimer and CrCu<sub>6</sub>-B, with two trinuclear Cu<sub>3</sub> entities. We deal first with the CrCu<sub>6</sub>-A derivative. The  $\chi_M T$  value increases continuously from room temperature to 2 K (Figure 9). This is consistent with a ferromagnetic interaction between the Cr<sup>III</sup> and the Cu<sup>II</sup> ions, in agreement with the orthogonality of the Cr<sup>III</sup> ( $t_{2g}$ )<sup>3</sup> and the Cu<sup>II</sup> ( $a_{1g}$ ) singly occupied orbitals, as predicted by Kahn's model and discussed later. The value of  $\chi_M T$  at 300 K is 5.4 cm<sup>3</sup> mol<sup>-1</sup> K (significantly higher than what is expected for the magnetically isolated spins: 4.125 cm<sup>3</sup> mol<sup>-1</sup> K with  $g=2$ ). At temperatures below 15 K,  $\chi_M T$  reaches a plateau and becomes 12.3 cm<sup>3</sup> mol<sup>-1</sup> K, which is the exact expected value for  $S=9/2$  (12.375 cm<sup>3</sup> mol<sup>-1</sup> K,  $g=2$ ). The  $\chi_M T$  experimental data were fitted to the analytical expression using the spin Hamiltonian given in Equation (1) and including a mean field correction  $zJ'$  for intermolecular interaction ( $z$  being the number of neighbours). The intramolecular interaction between the next nearest neighbours Cu<sup>II</sup> cations is neglected and the ground state zero field splitting  $D$  is expected to be zero. With an agreement factor  $R=1.1 \times 10^{-3}$ , the best-fit values give an exchange coupling value  $J=+45.5$  cm<sup>-1</sup>, a

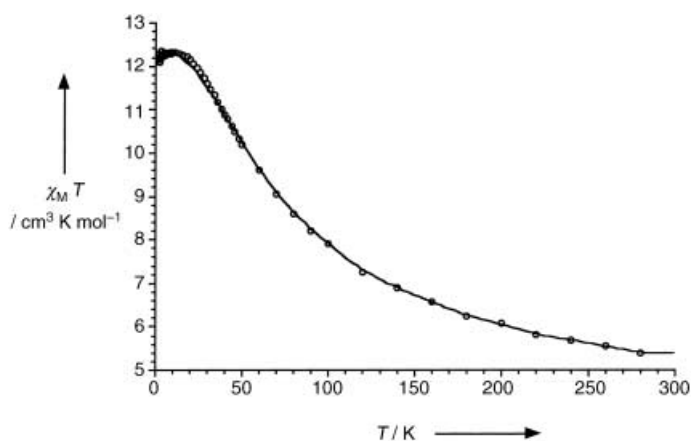


Figure 9. Thermal dependence of the  $\chi_M T$  for CrCu<sub>6</sub>.

Lande factor,  $g=1.99$ , an intermolecular interaction  $zJ'=1.5 \times 10^{-3}$  cm<sup>-1</sup> and  $D \sim 0$  cm<sup>-1</sup>. The  $J$  value is high compared to exchange coupling in other heterodimetallic  $\mu$ -cyano species.

The magnetisation as a function of the applied magnetic field, at 2 K, is reported in Figure 10. The data shows a value close to saturation at 9  $\mu_B$  and gives a further demonstration of

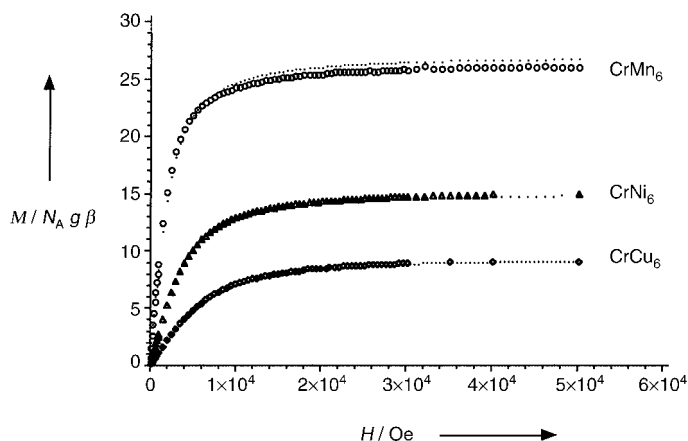


Figure 10. Field dependence of the magnetisation at 2 K for CrCu<sub>6</sub>, CrNi<sub>6</sub> and CrMn<sub>6</sub>; the dotted lines correspond to the Brillouin functions for  $S=9/2$ ,  $S=15/2$  and  $S=27/2$ .

the ground spin state,  $S=9/2$ . The good agreement of the data with the computed Brillouin function for a spin  $S=9/2$  shows that the ground state is the only one populated at  $T=2$  K. The energy of the first excited state computed by using the Hamiltonian given in Equation (1) is  $\Delta E/K = J \times (3/2k) \sim 98$  corresponds to this observation.

Table 4. Best-fitted values for parameters  $J$ ,  $g$ ,  $D$ , and,  $zJ'$  for all the complexes.

	IR: $\nu_{\text{CN}}$ [cm <sup>-1</sup> ]	$\theta$ , M-C-N [°]	$J$ exp. [cm <sup>-1</sup> ]	$g$	$zJ'$ [cm <sup>-1</sup> ]	$D$ [cm <sup>-1</sup> ]	R
CrCu <sub>6</sub>	2180	176.45	45.5	1.99	-0.001	-0.009	$1 \times 10^{-4}$
CrNi <sub>6</sub>	2149	164.6	17.3	1.96	-0.020	-0.029	$5 \times 10^{-4}$
CrMn <sub>6</sub>	2146	161.8 & 153.6	-9.0	1.98	-0.035	-0.042	$9 \times 10^{-5}$
CoCu <sub>6</sub>	2181	178.5	-0.82	2.10	-	-	$1 \times 10^{-5}$
CoNi <sub>6</sub>	1952	-	-0.45	2.00	0.005	-	$1.6 \times 10^{-3}$
CoMn <sub>6</sub>	2146	166.6 & 154.7	-0.15	1.98	0.002	-	$2.4 \times 10^{-3}$

The results obtained for the sample CrCu<sub>6</sub> (B-form), in the presence of trinuclear Cu<sub>3</sub> complex are in agreement with the previous data. To get the magnetic susceptibility of the heptanuclear complex [Cr(CN–Cu)<sub>6</sub>]<sup>9+</sup> in the CrCu<sub>6</sub>-B sample, we withdrew the experimental paramagnetic contribution of the trinuclear complex, [tren{Cu(tren)}<sub>3</sub>]<sup>6+</sup> (corresponding to the Curie law for three isolated spin 1/2 copper(II) from the experimental susceptibility of CrCu<sub>6</sub>-B. The resultant  $\chi_M T$  curve is similar to the one obtained for the CrCu<sub>6</sub>-A sample and the fit leads to similar  $J$ ,  $g$  and  $zJ'$  values. For the magnetisation as a function of the applied magnetic of the sample CrCu<sub>6</sub>-B, the data were obtained by withdrawing from the experimental magnetisation of CrCu<sub>6</sub> the magnetisation of six independent  $S = 1/2$  (six Cu<sup>II</sup> ions from the two parasitic trinuclear complexes), computed by the corresponding Brillouin function. The resulting magnetisation curve is similar to the one obtained for CrCu<sub>6</sub>-A and corresponds to  $S = 9/2$ .

**Magnetic properties of CrNi<sub>6</sub>:** Similar experiments and analyses have been performed for the CrNi<sub>6</sub> complex. The results are given in Table 4. For this compound, the treatment of the data is easier than for CrCu<sub>6</sub> since 1) there is no cocrystallised species in the compound and 2) there is a unique [Cr{CN–Ni(tetren)}<sub>6</sub>]<sup>9+</sup> entity in the unit cell.

The  $\chi_M T$  versus temperature curve (Figure 11) indicates that  $\chi_M T$  increases continuously as the temperature decreases until 6 K, characteristic of ferromagnetic behaviour, as foreseen by the orbital model. Below this temperature, the thermal dependence of  $\chi_M T$  mildly declines, an effect that

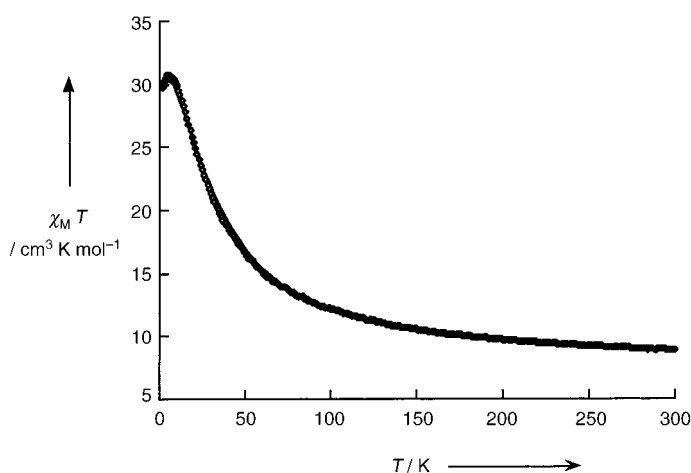


Figure 11. Thermal dependence of the  $\chi_M T$  product for CrNi<sub>6</sub>.

might be due to weak intermolecular interactions or zero-field splitting. The  $\chi_M T$  value obtained at high temperature is 8.93 cm<sup>3</sup> mol<sup>-1</sup> K, which is higher than the evaluation for six isolated paramagnetic nickel ions and an additive chromium atom (7.875 cm<sup>3</sup> mol<sup>-1</sup> K). At low temperature (6 K), the agreement between the experimental  $\chi_M T$  data (30.7 cm<sup>3</sup> mol<sup>-1</sup> K) and the theoretical value for  $S = 15/2$  (31.875 cm<sup>3</sup> mol<sup>-1</sup> K) is acceptable, considering the assumed intermolecular interactions. The  $\chi_M T$  experimental data were fitted to the theoretical expression coming from the Hamiltonian given in Equation (1) and lead to a coupling exchange

value  $J = +17.3$  cm<sup>-1</sup>, with  $g = 1.98$ , a sign of a quite strong ferromagnetic interaction between paramagnetic centres 5.27 Å apart and bearing two and three spins.

Addition of anisotropy  $D$  or intermolecular interaction terms in the fit do not allow significant improvement of the quality of the fit and lead to small values of  $D$  (–0.03 cm<sup>-1</sup>) or  $zJ'$  ( $5.8 \times 10^{-4}$  cm<sup>-1</sup>). The very low values simply confirm the high symmetry of the complex (weak anisotropy) and that the highly charged species are well isolated from each other, as anticipated from the synthetic strategy. The relatively high  $J$  value, in comparison with other “Cr–Ni” compounds such as trinuclear CrNi<sub>2</sub> complexes in which  $J = +10$  cm<sup>-1</sup>, might be explained by the weak distortion of the cyano bridge. Magnetostructural correlation in CrNi species is discussed in Part 3 of this series of papers.<sup>[19]</sup>

The magnetisation as a function of the applied magnetic field, at 2 K is reported in Figure 10. It corresponds to the unique [Cr{CN–Ni(tetren)}<sub>6</sub>]<sup>9+</sup> entity and displays a value close to saturation at 14.95 μ<sub>B</sub> (14.85 with  $g = 1.98$ ), confirmation of the ground spin state,  $S = 15/2$ . The agreement of the data with the computed Brillouin function for a spin  $S = 15/2$  shows that, at  $T = 2$  K, only the ground state is populated, in agreement with the energy of the first excited state computed using the Hamiltonian given in Equation (1):  $\Delta E/K = J \times (3/2k) \sim 37$ .

**Magnetic properties of CrMn<sub>6</sub>:** With respect to the CrMn<sub>6</sub> compound, the analysis takes into account the presence of two manganese(II) mononuclear complexes and two different [Cr{CN–Mn(tetren)}<sub>6</sub>]<sup>9+</sup> entities per unit cell. The two species [Cr{CN–Mn(tetren)}<sub>6</sub>]<sup>9+</sup> differ by the distortion of the cyano bridge and may present two different  $J$  values. To get the thermal variation of  $\chi_M T$  shown in Figure 12, which corresponds to only one heptanuclear complex [Cr{CN–Mn(tetren)}<sub>6</sub>]<sup>9+</sup>, we divided by two and subtracted the paramagnetic contribution of [Mn<sup>II</sup>(tetren)(H<sub>2</sub>O)]<sup>2+</sup> (Curie law for  $S = 5/2$ ) from the experimental susceptibility of the compound CrMn<sub>6</sub>. The  $\chi_M T$  value at room temperature is slightly smaller than the one computed for six insulated  $S = 5/2$  [Mn<sup>II</sup>] ions and one isolated  $S = 3/2$  [Cr<sup>III</sup>] ion (26.23 instead of 28.125 ~ 225/8 cm<sup>3</sup> mol<sup>-1</sup>). It decreases with temperature down to  $\chi_M T = 25.07$  at  $T = 148$  K and then increases steadily up to a maximum value of  $\chi_M T = 90.4$  at  $T = 2$  K. The presence

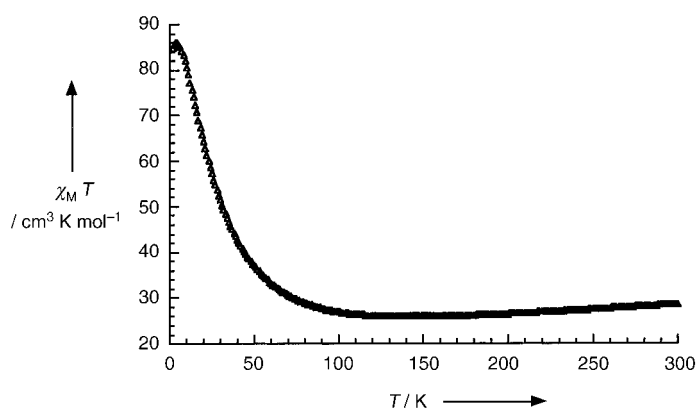


Figure 12. Thermal dependence of the  $\chi_M T$  product for CrMn<sub>6</sub>.

of the minimum is well documented<sup>[16]</sup> and is a characteristic signature of an antiferromagnetic coupling between spins of different values: here, in a  $[\text{Cr}(\text{CN}-\text{Mn}(\text{tetren}))_6]^{9+}$  unit, it means that the chromium(III) is antiferromagnetically coupled to the six manganese(II) ions, leading to a ground spin state  $S = 27/2$ . The  $\chi_M T$  value at the lowest available temperature is weaker than the expected value for spin  $S = 27/2$  with  $g = 2$  ( $\chi_M T = 97.875 \text{ cm}^3 \text{ mol}^{-1} \text{ K}$ ) but below 4 K  $\chi_M T$  reaches a plateau and then decreases, which might be the sign of an intermolecular interaction. To fit the susceptibility data, we first used the simplified Hamiltonian given in Equation (1) and got average values for  $J$  and  $g$ :  $J = -9 \text{ cm}^{-1}$  and  $g = 1.98$ . The  $J$  value confirms the antiferromagnetic interaction between chromium and manganese. A second fit taking into account the presence of two different  $[\text{Cr}\{\text{CN}-\text{Mn}(\text{tetren})\}_6]^{9+}$  species gave:  $J_1 = -7.2 \text{ cm}^{-1}$ ,  $J_2 = -10.8 \text{ cm}^{-1}$  and a mean  $g = 1.98$ . The two  $J$  values can be associated with the two different angles in the two  $[\text{Cr}(\text{CN}-\text{Mn})_6]^{9+}$   $\text{CrMn}_6$  with  $\theta = 161.7^\circ$  and  $\theta = 153.6^\circ$ : the larger  $J$  value corresponds to the larger angle (smaller deviation from linearity) and to a better overlap between the  $t_{2g}$  orbitals of chromium and manganese.

The magnetisation as a function of the applied magnetic field at 2 K is reported in Figure 10. It corresponds to one  $[\text{Cr}\{\text{CN}-\text{Mn}(\text{tetren})\}_6]^{9+}$  entity (dividing by two the experimental value and then subtracting the Brillouin contribution of the mononuclear  $[\text{Mn}^{\text{II}}(\text{tetren})(\text{H}_2\text{O})]^{2+}$  ion. At high field, it displays a value a little smaller than the saturation at  $27 \mu_B$ , (26.73 with  $g = 1.98$ ) in agreement with the large ground spin state,  $S = 27/2$ . The agreement of the experimental data with the computed Brillouin function for a spin  $S = 27/2$  and  $g = 1.98$  (from the fit of the susceptibility data) shows that, at  $T = 2 \text{ K}$ , the ground state is fully populated and that the first excited spin states do not contribute to the magnetic properties. Indeed, the energy of the first excited state computed by using the Hamiltonian given in Equation (1) is:  $\Delta E/K = |J| \times (3/2k) \sim 19.5$ .

**Magnetostructural correlation:** It is possible at this point to come back to the orbital mechanism leading to the nature, ferro- or antiferromagnetic, of the interaction between the chromium and its nearest neighbours, copper(II), nickel(II) and manganese(II), which can be foreseen by our simple orbital model. The exchange interactions are short range. The interpretation can be made at the simplest level, looking at the pairs  $\text{Cr}^{\text{III}} - \text{Cu}^{\text{II}}$ ,  $\text{Cr}^{\text{III}} - \text{Ni}^{\text{II}}$  and  $\text{Cr}^{\text{III}} - \text{Mn}^{\text{II}}$  and considering an ideal linear configuration of the Cr-CN-M bridge, the direction of which can be chosen as the  $z$  axis. In this framework, on the chromium side, the singly occupied molecular orbitals centred on the metal and partially delocalised on the cyanide ligand active in the exchange ("magnetic orbitals") are  $xz$  and  $yz$ , of local  $t_{2g}$  symmetry, or  $\pi$  symmetry related to the  $z$  axis. The  $xy$  orbital, the axes of which are in a plane perpendicular to the  $z$  axis, plays a lesser role for this particular Cr-M pair. On the M side, the  $z^2$  orbital belongs to  $\sigma$  symmetry related to the  $z$  axis and is therefore orthogonal to the chromium  $xz$  and  $yz$  orbitals. This is the origin of the ferromagnetism in  $\text{CrCu}_6$  and  $\text{CrNi}_6$ . In  $\text{CrNi}_6$ , the second magnetic orbital,  $x^2 - y^2$ , will also play a less

important role. The mechanism of the ferromagnetic interaction between  $\text{Cr}^{\text{III}}$  and  $\text{Cu}^{\text{II}}$  and  $\text{Ni}^{\text{II}}$  is the same as in the three-dimensional Prussian blue analogues.<sup>[56]</sup> The importance of the  $J$  value is related to the strong spin density overlap on the cyano bridge and particularly on the nitrogen atom: the Cr-CN-Cu(Ni) bridge is close to linearity: Cr-C-N angle =  $176.4^\circ$  and C-N-Cu(Ni) angle is  $176.5^\circ$  ( $164.6^\circ$ ). Thus, a strong spin density in  $\pi$ -symmetry orbitals (coming from  $\text{Cr}^{\text{III}}$ ) and a strong spin density in  $\sigma$  orbitals (coming from  $\text{Cu}^{\text{II}}$  or  $\text{Ni}^{\text{II}}$ ) are present on the nitrogen atom. The overlap density (product of these orbitals) is important around the nitrogen center and determines the value of the exchange integral  $k$  and therefore  $J = 2k$ . We shall see in detail later, in Part 3 of this series,<sup>[19]</sup> that the bridging angles play an important role in fixing the magnitude of the ferromagnetic interaction in  $\mu$ -cyanochromium-nickel complexes. As for  $\text{CrMn}_6$ , there are  $\sigma$ -symmetry orbitals on the manganese side like in the nickel case, and also  $\pi$  symmetry  $t_{2g} xz$  and  $yz$  orbitals. The first give a ferromagnetic contribution and the latter overlap with those of chromium, and give rise to an antiferromagnetic contribution that counterbalances and overcomes the ferromagnetic contribution and ensures the antiferromagnetic coupling between chromium and manganese. It is possible to compare the overall interaction energies  $J n_M n_{M'}$  ( $n_M$  = number of unpaired electrons on M,  $n_{M'}$  = number of unpaired electrons on  $M'$ ) corresponding to all the  $n_M n_{M'}$  orbital pathways:  $J n_{\text{Cr}} n_{\text{Cu}} = J \cdot 3 \cdot 1 = 135 \text{ cm}^{-1} \sim 196 \text{ K}$  ( $n_{\text{Cr}}$  = three unpaired electrons,  $n_{\text{Cu}}$  = one unpaired electron);  $J n_{\text{Cr}} n_{\text{Ni}} = J \cdot 3 \cdot 2 = 104 \text{ cm}^{-1} \sim 132 \text{ K}$  ( $n_{\text{Cr}}$  = three unpaired electrons,  $n_{\text{Ni}}$  = two unpaired electrons),  $J n_{\text{Cr}} n_{\text{Mn}} = |J| \cdot 3 \cdot 5 = 135 \text{ cm}^{-1} \sim 196 \text{ K}$  ( $n_{\text{Cr}}$  = three unpaired electrons,  $n_{\text{Mn}}$  = five unpaired electrons). The overall energy is so far not similar in the three compounds.

**Hexacyanocobaltate(III) derivatives:** To evidence and better understand the nature of the interaction between external metal ions ("second neighbours" or "next-nearest neighbours" interaction) at a distance through the centre larger than  $10 \text{ \AA}$ , we studied three heptanuclear complexes formed with a diamagnetic  $\text{Co}^{\text{III}}$  ion centre:  $\text{CoCu}_6$ ,  $\text{CoNi}_6$  and  $\text{CoMn}_6$ . The main results are reported in Table 4.

For the  $\text{CoCu}_6$  compound, the thermal dependence of  $\chi_M T$  is characteristic of a paramagnetic species.  $\chi_M T$  is constant with an experimental value of  $2.33 \text{ cm}^3 \text{ mol}^{-1} \text{ K}$  in agreement with six isolated copper(II) metallic ions (2.36 for six separated spin  $1/2$  and  $g = 2.1$ ). At low temperature, below 40 K, the  $\chi_M T$  curve decreases indicating either intra- and/or intermolecular antiferromagnetic interactions between the spin carriers. The value reached at 2 K is  $1.14 \text{ cm}^3 \text{ mol}^{-1} \text{ K}$  and extends to zero at lower temperature.

Concerning the  $\text{CoNi}_6$  and the  $\text{CoMn}_6$  complexes, similar magnetic behaviour is observed with a constant  $\chi_M T$  value at 5.83 and  $23.6 \text{ cm}^3 \text{ mol}^{-1} \text{ K}$ , respectively, expected for paramagnetic species but smaller than the calculated values for six isolated  $\text{Mn}^{\text{II}}$  ( $\chi_M T = 6 \text{ cm}^3 \text{ mol}^{-1} \text{ K}$ ) or for six isolated  $\text{Ni}^{\text{II}}$  ions ( $\chi_M T = 26.5 \text{ cm}^3 \text{ mol}^{-1} \text{ K}$ ). At low temperature,  $\chi_M T$  drops below 10 K, which indicates clearly intermolecular antiferromagnetic interaction between the spin carriers.

The values of the computed exchange coupling,  $-0.82$ ,  $-0.45$  and  $-0.15 \text{ cm}^{-1}$  for  $\text{CoCu}_6$ ,  $\text{CoNi}_6$  and  $\text{CoMn}_6$ , respectively, indicate that the next-nearest neighbours exchange interaction (through the  $\text{NC-Co}^{\text{III}}\text{-CN}$  bridge) is weak (compared to the nearest neighbours one) and that this parameter might be omitted in the magnetic studies of high-spin chromium-centred complexes, as done previously.

**Low-temperature experiments:** Preliminary experiments performed at low temperature (from 30 mK to 2 K) on the present  $\text{CrNi}_6$  high-spin complex indicate that no hysteresis loop and no frequency dependence of the AC susceptibility, characteristic of single-molecule magnet behaviour, are observed. This is due to the fact that the zero field splitting factor  $D$  is nearly zero, leading to a very small energy barrier between the two  $M_S$  spin states. Despite the high-spin value of the complex ( $S=15/2$ ), a relatively high  $J$  value ( $J=17.3 \text{ cm}^{-1}$ ) and no intermolecular interactions, the complex does not behave as a single-molecule magnet, indicating clearly the importance of the anisotropic factor for the observation of the expected physical properties.

Similar experiments have been performed on  $\text{CrNi}_6^*$ , a compound obtained from the tetren ligand of technical quality. A hysteresis loop at 300 mK is observed that is described elsewhere<sup>[57]</sup> and the nature of which is still controversial. The mixture of the polyamine ligands present in the sample may induce a disorder that might be associated with a slight structural anisotropy of the final complex, generating anisotropy. Concerning the  $\text{CrMn}_6$  complex, once again the studies at very low temperature indicate clearly that there is no single-molecule magnet behaviour. Nevertheless, these results allow a better understanding of the parameters required to obtain single-molecule magnet behaviour: the ground state spin value as well as the structural and electronic anisotropy.

## Conclusion

A rational synthetic strategy for highly charged polynuclear species, based on  $\text{Cr}^{\text{III}}$  and  $\text{Co}^{\text{III}}$  polycyanides, surrounded by  $\text{Cu}^{\text{II}}$ ,  $\text{Ni}^{\text{II}}$  and  $\text{Mn}^{\text{II}}$ , which might be extended to other metallic polycyanometalate precursors, has been described herein. High-spin molecules such as  $\text{CrCu}_6$  ( $S=9/2$ ),  $\text{CrNi}_6$  ( $S=15/2$ ) and  $\text{CrMn}_6$  ( $S=27/2$ ) and the corresponding cobalt(III)-centred species were thus synthesised and fully characterised. Despite the fact that  $\text{CrCu}_6$ ,  $\text{CrNi}_6$  and  $\text{CrMn}_6$  complexes are very isotropic and that no single-molecule magnet behaviour has been observed, these high-spin molecules might be of great interest. First of all, they open up a large family of polycyanometalate complexes of various nuclearities. New building blocks have been employed, especially the  $[\text{Mn}(\text{tetren})]^{2+}$  fragment, which has been used successfully and mentioned here for the first time. The polynuclear complexes described herein allow us to define and to better understand the chemical parameters involved in the field of single-molecule magnets and to design new chemical objects of potential interest. The study of isotropic high-spin molecules might be also interesting for physicists because it

provides new magnetic tools for the study of higher order parameters implied in the spin Hamiltonian. Finally, the possible control of the ground state spin value has been demonstrated, a necessity in the domain of nanomagnets. Another important parameter is the structural anisotropy that is analysed and controlled in Part 2<sup>[18]</sup> of this series of papers.

## Experimental Section

**Warning!** Although we have experienced no difficulties with the complexes described herein as perchlorate salts, these are potentially explosive and should be handled in small amounts and with great caution. We used them since no similar products or no crystals suitable for single crystal X-ray diffraction were obtained with other counterions.  $\text{K}_3[\text{Cr}(\text{CN})_6]$  was synthesised according to references [58, 59]. All other reagents were purchased as reagent grade chemicals and used without further purification. All solvents were of analytical grade quality. Air-sensitive products were synthesised using Schlenk techniques under an argon atmosphere, then transferred in a glove-box (a few ppm of dioxygen in aqueous atmosphere) and crystallised by slow evaporation of the solvent.

**$[\text{Cr}(\text{CN}-\text{Cu}(\text{tren}))_6](\text{ClO}_4)_9$  ( $\text{CrCu}_6\text{-A}$ ):** A solution of tris(2-amino)ethylamine (0.95 g, 6.5 mmol) in water–acetonitrile (1:1, 10 mL) was added to a solution of copper perchlorate (2.29 g, 6 mmol) in water–acetonitrile (1:1, 20 mL). The mixture was stirred for 5 min before hexacyanochromate(II) potassium salt (0.260 g, 0.8 mmol) dissolved in a minimum of water was added. The solution was left standing for 24 h and the fine blue hexagonal crystals formed were collected and washed with ethanol (a green precipitate was then eliminated by suction). Yield 32%. IR (KBr):  $\tilde{\nu}=2180 \text{ cm}^{-1}$  ( $\nu_{\text{as}}(\text{CN})$ ); elemental analysis calcd (%) for  $\text{C}_{42}\text{H}_{108}\text{Cl}_9\text{CrCu}_6\text{N}_{30}\text{O}_{36}$ : C 21.36, H 4.61, N 17.79, Cr 2.20, Cu 15.21, Cl 13.51; calcd for  $\text{C}_{42}\text{H}_{108}\text{Cl}_9\text{CrCu}_6\text{N}_{30}\text{O}_{36}(\text{CH}_3\text{CN})_2(\text{H}_2\text{O})_6$ : C 21.42, H 4.92, N 17.37, Cr 2.02, Cu 14.78, Cl 12.64; found: C 21.08, H 4.77, N 17.66, Cr 1.96, Cu 14.42, Cl 12.68.

**$[\text{Cr}(\text{CN}-\text{Cu}(\text{tren}))_6][\text{tren}\{\text{Cu}(\text{tren})\}_3]_2(\text{ClO}_4)_{21}$  ( $\text{CrCu}_6\text{-B}$ ):** A solution of tris(2-amino)ethylamine (0.95 g, 6.5 mmol) in water–acetonitrile (1:1, 10 mL) was added to a solution of copper perchlorate (2.29 g, 6 mmol) in water–acetonitrile (1:1, 30 mL). The mixture was stirred for 20 min before hexacyanochromate(III) potassium salt (0.325 g, 1 mmol) dissolved in a minimum of water was added. The solution was left standing for a few days and the blue hexagonal crystals formed were collected and washed with ethanol. Yield 78%. IR (KBr):  $\tilde{\nu}=2180 \text{ cm}^{-1}$  ( $\nu_{\text{as}}(\text{CN})$ ); elemental analysis calcd (%) for  $\text{C}_{90}\text{H}_{252}\text{CrCu}_{12}\text{N}_{62}\text{Cl}_{21}\text{O}_{84}$ : C 21.17, H 4.94, N 17.01, Cr 1.02, Cu 14.93, Cl 14.58; found: C 21.28, H 5.03, N 16.87, Cr 1.07, Cu 14.84, Cl 14.63.

**$[\text{Co}(\text{CN}-\text{Cu}(\text{tren}))_6](\text{ClO}_4)_9$  ( $\text{CoCu}_6\text{-A}$ ) and  $[\text{Co}(\text{CN}-\text{Cu}(\text{tren}))_6][\text{tren}\{\text{Cu}(\text{tren})\}_3]_2(\text{ClO}_4)_{21}$  ( $\text{CoCu}_6\text{-B}$ ):** A solution of tris(2-amino)ethylamine (0.95 g, 6.5 mmol) in water–acetonitrile (1:1, 10 mL) was added to a solution of copper perchlorate (2.29 g, 6 mmol) in water–acetonitrile (1:1, 20 mL). The mixture was stirred for 20 min before hexacyanocobaltate(III) potassium salt (0.2 g, 0.6 mmol) dissolved in a minimum of water was added. The solution was left standing for a few days, which led to two fractions of different crystals: fragile blue hexagonal plates ( $\text{CoCu}_6\text{-A}$ ; 51% yield) and deep blue hexagonal crystals ( $\text{CoCu}_6\text{-B}$ ; 15% yield) which are the expected heptanuclear complexes without (A) and with (B) a cocrystallised trinuclear copper(II) complex.

**A- $[\text{Co}(\text{CN}-\text{Cu}(\text{tren}))_6](\text{ClO}_4)_9$ :** IR (KBr):  $\tilde{\nu}=2188 \text{ cm}^{-1}$  (CN asymmetric stretch); elemental analysis calcd (%) for  $[\text{C}_{42}\text{H}_{108}\text{CoCu}_6\text{N}_{30}\text{Cl}_9\text{O}_{36}]$ : C 21.30, H 4.60, N 17.74, Co 2.49, Cu 16.10, Cl 13.47; calcd (%) for  $\text{C}_{42}\text{H}_{108}\text{CoCu}_6\text{N}_{30}\text{Cl}_9\text{O}_{36}(\text{CH}_3\text{CN})_2(\text{H}_2\text{O})_6$ : C 21.59, H 4.96, N 17.52, Co 2.30, Cu 14.90, Cl 12.47; found: C 20.95, H 5.10, N 16.95, Co 1.93, Cu 13.85, Cl 12.85.

**B- $[\text{Co}(\text{CN}-\text{Cu}(\text{tren}))_6][\text{tren}\{\text{Cu}(\text{tren})\}_3]_2(\text{ClO}_4)_{21}$ :** IR (KBr):  $\tilde{\nu}=2188 \text{ cm}^{-1}$  ( $\nu_{\text{as}}(\text{CN})$ ); elemental analysis calcd (%) for  $\text{C}_{90}\text{H}_{252}\text{CoCu}_{12}\text{N}_{62}\text{Cl}_{21}\text{O}_{84}$ : C 21.14, H 4.97, N 16.98, Co 1.15, Cu 14.91, Cl 14.56; found: C 20.95, H 5.11, N 17.15, Co 1.05, Cu 14.68, Cl 14.66.

**$[\text{tren}\{\text{Cu}(\text{tren})\}_3](\text{ClO}_4)_6$ :** A solution of tris(2-amino)ethylamine (1.17 g, 8 mmol, 4/3 equiv) in water–acetonitrile (1:1, 10 mL) was added to a solution of copper(II) perchlorate (2.29 g, 6 mmol) in water–acetonitrile

(1:1, 30 mL). The mixture was stirred for 20 min and then left standing for a few days. The blue crystals were collected and washed with ethanol. Yield 95%. Elemental analysis calcd (%) for  $C_{24}H_{72}Cu_3N_{16}Cl_6O_{24}$ : C 21.01, H 5.29, N 16.33, Cu 13.89, Cl 15.50; calcd for  $C_{24}H_{72}Cu_3N_{16}Cl_6O_{24} \cdot (CH_3CN)$ : C 22.10, H 5.35, N 16.85, Cu 13.49, Cl 15.05; found: C 22.35, H 5.70, N 17.96, Cu 14.00, Cl 14.52.

**[Cr{CN–Ni(tetren)}<sub>6</sub>(ClO<sub>4</sub>)<sub>9</sub>(H<sub>2</sub>O)<sub>2</sub> (CrNi<sub>6</sub>)**: Potassium hydroxide (850 mg, 5.6 mmol) in aqueous solution followed by nickel(II) perchlorate (755 mg, 2 mmol) dissolved in a minimum of water were added to a solution of tetren · 5HCl (tetraethylene pentamine pentahydrochloride) (1.12 g, 3.01 mmol) dissolved in water (20 mL). The mixture was stirred for 10 min before solid silver perchlorate (3.12 g, 3.01 mmol) was added to eliminate the chloride ions. The solution was left stirring for 1 h in the dark, then the precipitate was filtered off and acetonitrile (20 mL) was added to the resulting filtrate. Hexacyanochromate(III), potassium salt (0.150 g, 0.46 mmol) dissolved in a minimum of water was added and the solution left standing for a few days in the presence of a large excess of sodium perchlorate salt (2 g). The red-purple octahedral crystals formed were collected and washed with water. 82% Yield; IR (KBr):  $\tilde{\nu} = 2149 \text{ cm}^{-1}$  ( $\nu_{as}(\text{CN})$ ); UV/Vis (H<sub>2</sub>O/CH<sub>3</sub>CN):  $\lambda_{max}(\epsilon) = 791(65), 537(33), 337 \text{ nm}(202)$  (L mol<sup>-1</sup> cm<sup>-1</sup>); elemental analysis calcd (%) for  $C_{54}H_{138}CrNi_6N_{36}Cl_9O_{36}(H_2O)_6$ : C 24.03, H 5.60, N 18.68, Cr 1.93, Ni 13.05, Cl 11.82; found: C 23.72, H 5.39, N 18.68, Cr 1.85, Ni 13.28, Cl 11.97.

**[Co{CN–Ni(tetren)}<sub>6</sub> (ClO<sub>4</sub>)<sub>9</sub> (CoNi<sub>6</sub>)**: Potassium hydroxide (1.7 g, 30 mmol) in aqueous solution followed by nickel(II) perchlorate (2 g, 6 mmol) dissolved in a minimum of water were added to a solution of tetren · 5HCl (tetraethylene pentamine pentahydrochloride) (2.23 g, 6 mmol) dissolved in water–acetonitrile (20 mL). The mixture was stirred for 10 min and then potassium hexacyanocobaltate(III) (0.331 g, 1 mmol) dissolved in a minimum of water was added and the solution left standing for a few days. The red-purple octahedral crystals formed were collected and washed with water. 52% Yield; IR (KBr):  $\tilde{\nu} = 2152 \text{ cm}^{-1}$  ( $\nu_{as}(\text{CN})$ ); elemental analysis calcd (%) for  $C_{54}H_{138}CoNi_6N_{36}Cl_9O_{36}$ : C 24.97, H 5.32, N 19.41, Co 2.27, Ni 13.56, Cl 12.28; found: C 25.45, H 5.49, N 19.26, Co 2.18, Ni 13.24, Cl 12.18.

**[Cr{CN–Mn(tetren)}<sub>6</sub>]<sub>2</sub> [Mn(tetren)(H<sub>2</sub>O)]<sub>2</sub> (ClO<sub>4</sub>)<sub>22</sub> (CrMn<sub>6</sub>)**: The experiment was performed in Schlenk tubes under an argon atmosphere (or in a glove box). Sodium hydroxide (0.3 g,  $7.5 \times 10^{-4}$  mol, 5 equiv) in aqueous solution followed by manganese(II) perchlorate (543 mg, 0.15 mmol, 1 equiv) in deoxygenated water (5 mL) were added to a solution of tetren · 5HCl (tetraethylene pentamine pentahydrochloride) (557 mg, 0.15 mmol) in water (10 mL). The mixture was stirred for 10 min before solid silver perchlorate (1.46 g, 7.5 mmol, 5 equiv) was added to precipitate the chloride ions. The solution was left stirring for one hour in the dark, then the precipitate was filtered off using a cannula, and acetonitrile (10 mL) was added to the resulting filtrate. Potassium hexacyanochromate(III) (0.084 g, 0.217 mmol, 1/6 equiv) dissolved in a minimum of water was added and the resulting pale yellow solution was left standing in a dioxxygen-free glove box. The orange-brown parallelepiped crystals formed were collected and washed with water. IR (KBr):  $\tilde{\nu} = 2146 \text{ cm}^{-1}$  ( $\nu_{as}(\text{CN})$ ); UV/Vis (H<sub>2</sub>O/CH<sub>3</sub>CN):  $\lambda_{max}(\epsilon) = 367 \text{ nm}(369 \text{ L mol}^{-1} \text{ cm}^{-1})$ ; elemental analysis calcd (%) for  $[C_{54}H_{138}CrMn_6N_{36}][Cl_{11}O_{44}][Mn_2C_8H_{25}N_5O]$ : C 24.58, H 5.42, N 18.95, Cr 1.72, Mn 12.69, Cl 12.87; found: C 24.58, H 5.56, N 18.87, Cr 2.04, Mn 12.19, Cl 13.44.

**[Co{CN–Mn(tetren)}<sub>6</sub>]<sub>2</sub> [Mn(tetren)(H<sub>2</sub>O)]<sub>2</sub> (ClO<sub>4</sub>)<sub>22</sub> (CoMn<sub>6</sub>)**: The experiment was performed following the procedure described for CrMn<sub>6</sub> using potassium hexacyanocobaltate(III) (0.084 g, 0.217 mmol, 1/6 equiv) instead of hexacyanochromate(III). The pale yellow solution was left standing in a glove box. The light yellow parallelepiped crystals formed were collected and washed with water. IR (KBr):  $\tilde{\nu} = 2146 \text{ cm}^{-1}$  ( $\nu_{as}(\text{CN})$ ); elemental analysis calcd (%) for  $[C_{54}H_{138}CoMn_6N_{36}][Cl_{11}O_{44}][Mn_2C_8H_{25}N_5O]$ : C 24.52, H 5.41, N 18.91, Co 1.94, Mn 12.66, Cl 12.84; found: C 24.37, H 5.50, N 18.76, Co 1.86, Mn 12.58, Cl 13.01.

**Physical characterisation**: IR spectra were recorded between 4000 and 250 cm<sup>-1</sup> on a Bio-Rad FTS 165 FT-IR spectrometer on KBr pellets. DC magnetic susceptibility measurements were carried out on a Quantum Design MPMS SQUID susceptometer equipped with a 5 T magnet and operating in the temperature range 1.8 to 400 K. The powdered samples (10–50 mg) were placed in a diamagnetic sample holder and the measurements realised in a 200 Oe applied field using the extraction technique.

Before analysis, the experimental susceptibility was corrected from diamagnetism using Pascal constants<sup>[61]</sup> and from temperature independent paramagnetism (TIP) of the transition metals.<sup>[60]</sup> Electrospray ionization mass spectrometry experiments were performed on an ESQUIRE ion trap (Bruker-Franzen Analytic GmbH, Bremen, Germany).<sup>[61]</sup> The non-linear ion trap worked in the mass-selective instability mode without using DC voltage (that is,  $U = 0$  condition) at the ring electrode. The instrument has a fundamental RF frequency of 781 kHz and is used in the standard mode: a mass-to-charge ratio up to 2000 Th with a selective resonance ejection at the non-linear resonance at 2/3 ( $q_z = 0.78$ ). The ion trap operated at an uncorrected partial He buffer gas pressure of  $3.4 \times 10^{-5}$  Torr ( $4.5 \times 10^{-3}$  Pa). A differentially pumped interface transferred the ions from the electrospray source (Analytica of Brandford, Inc., Brandford, CT) to the mass spectrometer. Some applied parameters were unchanged for all experiments, as the RF frequency amplitude of the hexapole (700 V), and the voltage applied to the electron multiplier (–1500 V). In the positive ion mode, the DC voltage applied to the ion guide (hexapole) was 2 V, the dynode voltage of the electron multiplier was –5 kV, the delay before scanning was 10 ms and the exit lens voltage was –100 V. The complexes were analysed after dilution at approximately  $10^{-4} \text{ mol l}^{-1}$  in dry acetonitrile or methanol/acetonitrile (5:1, v/v) and were infused into the ESI source using a Cole-Parmer Instrument Company (74900 series) syringe pump at a flow rate of 2  $\mu\text{L min}^{-1}$ . The capillary entry voltage was about –3500 V. The N<sub>2</sub> drying gas temperature was 150 °C with a flow rate of 200 L h<sup>-1</sup>.

**Crystallographic studies**: Suitable crystals for X-ray crystallography were obtained directly from the reaction medium or by re-crystallisation from water–acetonitrile solutions. For all the structures described herein, accurate cell dimensions and orientation matrices were obtained by least-squared refinements of 25 accurately centred reflections on a Nonius CAD4 diffractometer using graphite-monochromatic MoK $\alpha$  radiation. No significant variations were observed in the intensities of two checked reflections during data collections. Absorption corrections were applied by using the  $\psi$ -scan method. Refinement was performed by using the PC version of Crystals.<sup>[62]</sup> Scattering factors and corrections for anomalous dispersion were taken from Cromer.<sup>[63]</sup> The structures were solved with SHELX 86<sup>[64]</sup> followed by Fourier maps technique and refined by full-matrix least-squares with anisotropic thermal parameters for all non-hydrogen atoms, when sufficient data were available.

CCDC-184835 (CrCu<sub>6</sub>), CCDC-184838 (CrNi<sub>6</sub>), CCDC-184837 (CrMn<sub>6</sub>), CCDC-184840 (CoCu<sub>6</sub>), CCDC-184839 (CoMn<sub>6</sub>) and CCDC-184836 (Cu<sub>3</sub>) contain the supplementary crystallographic data for this paper. These data can be obtained free of charge via [www.ccdc.cam.ac.uk/conts/retrieving.html](http://www.ccdc.cam.ac.uk/conts/retrieving.html) (or from the Cambridge Crystallographic Center, 12 Union Road, Cambridge CB2 1EZ, UK; Fax: (+44) 1223-336033; or deposit@ccdc.cam.ac.uk).

## Acknowledgments

We thank Izio Rosenman, University Denis Diderot in Paris, for the Squid facilities, Talal Mallah for helpful discussions, Wolfgang Wernsdorfer for micro-Squid experiments and Carley Paulsen for low-temperature magnetic studies, not reported here. We thank the CNRS, the University Pierre et Marie Curie (Paris vi), the European Science Foundation (ESF) and the European Community for financial support (TMR No HPRN-CT199990012).

- [1] M. N. Leuenberger, D. Loss, *Nature* **2001**, *410*, 789–793.
- [2] L. Néel, *Ann Geophys.* **1949**, *5*, 99.
- [3] G. Christou, D. Gatteschi, D. N. Hendrickson, R. Sessoli, *MRS Bull.* **2000**, *25*(11), 66–71.
- [4] D. Gatteschi, A. Caneschi, L. Pardi, R. Sessoli, *Science* **1994**, *265*, 1054.
- [5] S. M. J. Aubin, M. W. Wemple, D. M. Adams, H.-L. Tsai, G. Christou, D. N. Hendrickson, *J. Am. Chem. Soc.* **1996**, *118*, 7746–7754.
- [6] T. Lis, *Acta Crystallogr. Sect. B* **1980**, *36*, 2042–2046.
- [7] R. Sessoli, D. Gatteschi, A. Caneschi, M. A. Novak, *Nature* **1993**, *365*, 141–143.

- [8] R. Sessoli, H.-L. Tsai, A. R. Schake, S. Wang, J. B. Vincent, K. Folting, D. Gatteschi, G. Christou, D. N. Hendrickson, *J. Am. Chem. Soc.* **1993**, *115*, 1804–1816.
- [9] D. N. Hendrickson, G. Christou, E. Ward, A. Schmitt, E. Libby, J. S. Bashkin, S. Wang, H. L. Tsai, J. B. Vincent, P. D. W. Boyd, J. C. Huffman, K. Folting, Q. Li, W. E. Streib, *J. Am. Chem. Soc.* **1992**, *114*, 2455–2471.
- [10] W. Wernsdorfer, N. Aliaga-Alcade, D. N. Hendrickson, G. Christou, *Nature* **2002**, *416*, 406–409.
- [11] D. Gatteschi, R. Sessoli, A. Cornia, *Chem. Commun.* **2000**, 725–732.
- [12] A. L. Barra, F. Bencini, A. Caneschi, D. Gatteschi, C. Paulsen, C. Sangregorio, R. Sessoli, L. Sorace, *ChemPhysChem* **2001**, *2*, 523–531.
- [13] L. Thomas, F. Lioni, R. Ballou, D. Gatteschi, R. Sessoli, B. Barbara, *Nature* **1996**, *383*, 145–147.
- [14] J. R. Friedman, M. P. Sarachik, J. Tejada, J. Maciejewski, R. Ziolo, *Phys. Rev. Lett.* **1996**, *76*, 3830–3833.
- [15] W. Wernsdorfer, R. Sessoli, *Science* **1999**, *284*, 133–135.
- [16] O. Kahn, *Molecular Magnetism*, Wiley-VCH, Weinheim, **1993**.
- [17] *Magnetism: Molecules to Materials* (Eds.: J. S. Miller, M. Drillon), Wiley-VCH, Weinheim, **2001**.
- [18] V. Marvaud, C. Decroix, A. Sculler, F. Tuyères, J. Vaissermann, C. Guyard-Duhayon, F. Gonnet, M. Verdaguer, *Chem. Eur. J.* **2003**, *9*, 1692–1705.
- [19] V. Marvaud, A. Sculler, F. Fabrizi de Biani, J. Vaissermann, C. Guyard-Duhayon, F. Tuyères, M. Verdaguer, unpublished results.
- [20] R. E. P. Winpenny, *J. Chem. Soc. Dalton Trans.* **2002**, 1–10.
- [21] C. Cadoui, M. Murrie, C. Paulsen, V. Villar, W. Wernsdorfer, R. E. P. Winpenny, *Chem. Commun.* **2001**, 2666–2667.
- [22] A. K. Powell, S. L. Heath, D. Gatteschi, L. Pardi, R. Sessoli, G. Spina, F. del Giallo, F. Piralli, *J. Am. Chem. Soc.* **1995**, *117*, 2491.
- [23] J. C. Goodwin, R. Sessoli, D. Gatteschi, W. Wernsdorfer, A. K. Powell, S. L. Heath, *J. Chem. Soc. Dalton Trans.* **2000**, 1835–1840.
- [24] Z. J. Zhong, H. Seino, Y. Mizobe, M. Hidai, A. Fujishima, S. Ohkoshi, K. Hashimoto, *J. Am. Chem. Soc.* **2000**, *122*, 2952–2953.
- [25] J. Larianova, M. Gross, M. Pilkington, H.-P. Anders, H. Stoeckli-Evans, H. U. Güdel, S. Decurtins, *Angew. Chem.* **2000**, *112*, 1667; *Angew. Chem. Int. Ed.* **2000**, *39*, 1605–1609.
- [26] M. Pilkington, S. Decurtins, *Chimia*, **2000**, *54*(10), 593–601.
- [27] M. Murrie, H. Stoeckli-Evans, H. U. Güdel, *Angew. Chem.* **2001**, *113*, 2011; *Angew. Chem. Int. Ed.* **2001**, *40*, 1957–1960.
- [28] S. Ferlay, T. Mallah, R. Ouahès, P. Veillet, M. Verdaguer, *Nature* **1995**, *378*, 701–703.
- [29] E. Dujardin, S. Ferlay, X. Phan, C. Desplanches, C. Cartier dit Moulin, P. Sainctavit, F. Baudelet, E. Dartyge, P. Veillet, M. Verdaguer, *J. Am. Chem. Soc.* **1999**, *121*, 6521–6521.
- [30] a) M. Verdaguer, A. Bleuzen, V. Marvaud, J. Vaissermann, M. Seuleiman, C. Desplanches, A. Sculler, C. train, G. Gelly, C. Lomenech, I. Rosenman, P. Veillet, C. Cartier dit Moulin, F. Villain, *Coord. Chem. Rev.* **1999**, *190*, 1023–1047; b) V. Marvaud, J. M. Herrera, T. Barilero, F. Tuyeras, R. Garde, A. Sculler, C. Decroix, M. Cantuel, C. Desplanches, *Monatshfte für Chemie* **2003**, *134*, 149–163.
- [31] T. Mallah, C. Auberger, M. Verdaguer, P. Veillet, *J. Chem. Soc. Chem. Commun.* **1995**, 61–62.
- [32] A. Sculler, T. Mallah, M. Verdaguer, A. Nivorozhkin, J.-L. Tholence, P. Veillet, *New J. Chem.* **1996**, *20*, 1–3.
- [33] R. J. Parker, D. C. R. Hockless, B. Moubaraki, K. S. Murray, L. Spiccia, *Chem. Commun.* **1996**, 2789–2790.
- [34] R. J. Parker, L. Spiccia, K. J. Berry, G. D. Fallon, B. Moubaraki, K. S. Murray, *Chem. Commun.* **2001**, 333.
- [35] R. J. Parker, L. Spiccia, S. R. Batten, J. D. Cashion, G. D. Fallon, *Inorg. Chem.* **2001**, *40*, 4696–4704.
- [36] Anonymous, *Miscellanea Berolinensia ad incrementum scientiarum (Berlin)* **1710**, *1*, 377.
- [37] J. F. Keggin, F. D. Miles, *Nature* **1936**, *137*, 577.
- [38] A. Ludi, H. U. Güdel, *Struct. Bonding* **1973**, *14*, 1.
- [39] A. G. Sharpe, *The chemistry of cyano complexes of the transition metals*, Academic Press, New York, **1976**, p 46, and references therein.
- [40] A. Rodríguez-Fortea, P. Alemany, S. Alvarez, E. Ruiz, A. Sculler, C. Decroix, V. Marvaud, J. Vaissermann, M. Verdaguer, I. Rosenman, M. Julve, *Inorg. Chem.* **2001**, *40*, 5868–5877.
- [41] P. J. Haÿ, J. C. Thibeault, R. Hoffmann, *J. Am. Chem. Soc.* **1975**, *97*, 4884.
- [42] J.-J. Girerd, Y. Journeaux, O. Kahn, *Chem. Phys. Lett.* **1981**, *82*, 534.
- [43] V. Marvaud, C. Decroix, J. Vaissermann, C. Guyard-Duhayon, M. Verdaguer, unpublished results.
- [44] D. A. House, *Coord. Chem. Rev.* **1977**, 257.
- [45] K. Weighardt, E. Schoffmann, B. Nuber, J. Weiss, *Inorg. Chem.* **1986**, *25*, 4877.
- [46] D. P. Riley, R. H. Weiss, *J. Am. Chem. Soc.* **1994**, *116*, 387.
- [47] a) K. Van Langenberg, S. R. Batten, K. J. Berry, D. C. R. Hockless, B. Moubaraki, K. S. Murray, *Inorg. Chem.* **1997**, *36*, 5006–5015; b) S. J. Brudenell, L. Spiccia, A. M. Bond, G. D. Fallon, D. C. R. Hockless, G. Lazarev, P. J. Mahon, E. R. T. Tiekink, *Inorg. Chem.* **2000**, *39*, 881–892.
- [48] I. P. Y. Shek, T.-C. Lau, W.-T. Wong, J.-L. Zuo, *New J. Chem.* **1999**, *23*, 1049.
- [49] This compound, interesting from an anisotropic and magnetic point of view ( $S=7/2$ ), is described in Part 3.<sup>[19]</sup>
- [50] a) K. Wieghardt, *Angew. Chem.* **1989**, *101*, 1179–1198; *Angew. Chem. Int. Ed. Engl.* **1989**, *28*, 1153–1172; b) K. Sauer, *Acc. Chem. Res.* **1980**, *13*, 249–256; c) G. W. Brudvig, H. H. Thorp, R. H. Crabtree, *Acc. Chem. Res.* **1991**, *24*, 311–316.
- [51] K. Nakamoto, *Infrared Spectra of Inorganic and Coordination compounds*, 2nd ed., Wiley Interscience, New York, **1970**, p. 179.
- [52] M. F. A. El-Sayed, R. K. Sheline, *J. Inorg. Nucl. Chem.* **1958**, *6*, 187.
- [53] a) J. O. Eriksen, A. Hazell, A. Jensen, J. Jepsen, R. D. Poulsen, *Acta Crystallogr. Sect. C* **2000**, *56*, 551; b) M. Ferbinleanu, S. Tanare, M. Andruh, Y. Journaux, F. Compoesu, I. Sheyer, E. Riviere, *Polyhedron* **1999**, *18*, 3019; c) M. Ohba, N. Usuki, N. Fukita, H. Okawxa, *Inorg. Chem.* **1998**, *37*, 3349.
- [54] J. H. Van Vleck, *The theory of electric and magnetic susceptibilities*, Oxford University Press, Oxford, **1932**.
- [55] a) A. Gleizes, M. Verdaguer, *J. Am. Chem. Soc.* **1984**, *105*, 3727–3737; b) M. Verdaguer, A. Gleizes, J. P. Renard, J. Seiden, *Phys. Rev. B* **1984**, *29*, 5144–5155.
- [56] V. Gadet, T. Mallah, I. Castro, P. Veillet, M. Verdaguer, *J. Am. Chem. Soc.* **1992**, *114*, 9213.
- [57] V. Marvaud, F. Tuyères, T. Mallah, C. Paulsen, W. Wernsdorfer, M. Verdaguer, unpublished results.
- [58] V. Marvaud, T. Mallah, M. Verdaguer, *Inorg. Synth.* in press.
- [59] S. Ferlay, T. Mallah, R. Ouahès, P. Veillet, M. Verdaguer, *Inorg. Chem.* **1999**, *38*, 229–234.
- [60] F. E. Mabbs, D. J. Machin, *Magnetism and Transition Metal Complexes*, Chapman and Hall, London, **1973**.
- [61] Y. Wang, M. Schubert and J. Franzen, *Proc. 44th ASMS Conf. Mass Spectrom. & Allied Topics*, Portland OR, **1996**, 131.
- [62] D. J. Watkin, J. R. Carruthers, P. W. Betteridge, *Crystals User Guide*, Chemical Crystallography Laboratory, University of Oxford, Oxford, UK, **1988**.
- [63] D. T. Cromer, *International Tables for X-ray Crystallography*, Vol. 1v, Kynoch, Birmingham, UK, **1974**.
- [64] G. M. Sheldrick, SHELXS 86, A Program for Crystal Structure Determination, University of Göttingen, Germany, **1986**.

Received: July 29, 2002

Revised: December 2, 2002 [F4296]